THESIS APPROVAL

GRADUATE SCHOOL, KASETSART UNIVERSITY

Master of Science (Genetics)

DEGREE

Genetics — **FIELD**

Genetics — **DEPARTMENT**

TITLE: Characterization of Membrane Binding Sites of *Bacillus thuringiensis* Cyt2Aa2 Toxin

NAME: Miss Pajaree Saitonuang

THIS THESIS HAS BEEN ACCEPTED BY

THESIS ADVISOR

(Mrs. AnchaneeKubera, Ph.D.)

THESIS CO-ADVISOR

(Assistant Professor BoonhiangPromdonkoy, Ph.D.)

DEPARTMENT HEAD

(Associate Professor ArinthipThamchaipenet, Ph.D.)

APPROVED BY THE GRADUATESCHOOL ON _____

DEAN

(Associate Professor GunjanaTheeragool, D.Agr.)

Copyright by Kasetsart University All rights reserved

THESIS

CHARACTERIZATION OF MEMBRANE BINDING SITES OF *BACILLUS THURINGIENSIS* CYT2AA2 TOXIN

PAJAREE SAITONUANG

A Thesis Submitted in Partial Fulfillment of
the Requirements for the Degree of
Master of Science (Genetics)
Graduate School, Kasetsart University
2015

Copyright by Kasetsart University All rights reserved

Pajaree Saitonuang 2015: Characterization of Membrane Binding Sites of *Bacillus thuringiensis* Cyt2Aa2 Toxin. Master of Science (Genetics), Major Field: Genetics, Department of Genetics. Thesis Advisor: Mrs. Anchanee Kubera, Ph.D. 71 pages.

Cyt2Aa2 is a cytolytic toxin produced from *Bacillus thuringiensis* subsp. *darmstadiensis*. It is specifically toxic against Dipteran larvae *in vivo*, and also active to several cell types such as erythrocytes**.** The active toxin is proposed to bind to cell membrane, leading to the formation of membrane pore by toxin oligomerization and eventually cell lysis. This study aimed to characterize the role of expected lipid binding residues (I139, S159, L160, S161, A162, D209 and V215) of Cyt2Aa2. Alanine scanning mutants were constructed by site-directed mutagenesis and expressed in *E. coli*. These mutants were expressed as inclusion bodies which were solubilized in 50 mM carbonate buffer pH 10.5. All mutants, except I139A and V215A could retain as activated toxins after proteinase K cleavage. Three mutants, S159A, L160A and S161A showed high hemolytic activity but low toxicity against *A. aegypti*. Membrane interaction assays showed that these mutants bound and formed complexes on rat red blood cells. Substitution by valine at A162 and asparagine at D209 could interfere membrane binding and oligomerization of the toxin. These mutants could not completely break RBC even at high concentration and showed no hemolytic activity. The mutant A162V showed no toxicity against *A. aegypti*, but D209N showed low toxicity against *A. aegypti*. Our data suggested that amino acids on loop between β4 and β5, and β7 of Cyt2Aa2 toxin were involved in membrane binding as well as complex formation. Substitution of amino acids in these regions altered the biological activity. Selectivity of the toxin to certain target cells might be improved by amino acid replacement in these regions.

_____ _____ __ / __ / ___

Student's signature Thesis Advisor's signature

Copyright by Kasetsart University All rights reserved

ACKNOWLEDGEMENTS

I would sincerely like grateful thanks and appreciate to King of Thailand due to The King is develope education in Thailand and opened Thai social to international. Wishing Long Live His Majesty The King.

I would sincerely like to grateful thanks and indebted to Dr. Anchanee Kubera, Department of Genetics, that my thesis advisor for her suggestion, encouragement, teaching to new skills and open my mind to new knowledge and opportunities. Also thanks to Assist. Prof. Boonhiang Promdonkoy, National Center for Genetic Engineering and Biotechnology (BIOTEC) for his suggestion and giving me the *E. coli* harboring *cyt2Aa2* wild type cell and anti-Cyt2Aa2 for using in this research.

I would like to thank Prof. Theeraphap Chareonviriyaphap, Department of Entomology, Faculty of Agriculture, Kasetsart University for allowing me rearing mosquito in his laboratory, also thanks to Department of Genetics and Department of microbiology, Faculty of Science, Kasetsart University for using good and comfortable to laboratory. I would like to give very special thanks like to all teachers of genetics, members of genetics, members of lab 4511, lab 4507, lab 4505 and lab AK, Chalintorn Wilaisorn, Chalalai Janekabuan, Amornrat Chaowai, Watcharakorn Mongkol and Nipaporn Deejai for their helpfulness, suggestion and relationship.

A special thanks to my close friend, Turkey friend and Chinese friend that there were encouraged, cheerfulness and pleased to my completely thesis. Finally, Federico Turcutto and My family which there are very important for supporting and helping to all everything along with teach me about patience to around environment. Thankfully and Love.

Pajaree Saitonuang

November, 2014

Copyright by Kasetsart University All rights reserved

TABLE OF CONTENTS

Page

Copyright by Kasetsart University. All rights reserved

LIST OF TABLES

Copyright by Kasetsart University All rights reserved

LIST OF FIGURES

Copyright by Kasetsart University All rights reserved

LIST OF FIGURES (Continued)

Appendix Figure

Copyright by Kasetsart University All rights reserved

LIST OF FIGURES (Continued)

Copyright by Kasetsart University All rights reserved

LIST OF ABBREVIATIONS

A.aegypti	=	*Aedes aegypti*
BSA	=	bovine serum albumin
Bt	=	*Bacillus thuringiensis*
Btd	=	*Bacillus thuringiensis* subsp. *darmstadiensis*
°C	=	degree Celcius
C-terminal	=	carboxy-terminal end
Cyt	=	cytolytic toxins
DMSO	=	dimethyl sulfoxide
DNA	=	deoxyribonucleic acid
dNTP	=	deoxyribonucleotide triphosphate
E. coli	=	*Escherichia coli*
EtBr	=	ethidium bromide
g	=	gravitational acceleration in relative centrifugal force
HCl	=	hydrochloric acid
IPTG	=	isopropylthio-β-galactoside
kb	=	kilo base pair
kDa	=	Kilogram Dalton
M	=	molar
mg	=	milligram
ml	=	milliliter
mM	=	millimolar
PFT	=	pore forming toxin
PMSF	=	phenylmethanesul- fonylfluoride
µg	=	microgram
µl	=	microliter
NaCl	=	sodium chloride
NCBI	=	National Center for Biotechnology Information
NCI	=	National Cancer Institute
nm	=	nanometer
N-terminal	=	amino-terminal end

Copyright by Kasetsart University All rights reserved

LIST OF ABBREVIATIONS (Continued)

PCR	=	Polymerase chain reaction
PDB	=	protein data bank
RBC	=	red blood cells
rpm	=	round per minute
SDW	=	steriled distilled water
Tris	=	tris (hydroxymethyl) aminomethane
UV	=	ultraviolet
VVA	=	volvatoxin A2

Copyright by Kasetsart University All rights reserved

CHARACTERIZATION OF MEMBRANE BINDING SITES OF BACILLUS THURINGIENSIS CYT2AA2 TOXIN

INTRODUCTION

Bacillus thuringiensis (*Bt*) is a gram-positive spore-forming bacterium that can produce δ-endotoxins during sporulation (Schnepf *et al.*, 1998). The life cycle of *Bt* is characterized by two phases which include vegetative cell division and spore development, otherwise referred to as the sporulation cycle (Bulla *et al.,* 1980). These toxins are first produced as an inactive protoxin, and then proteolytically processed into an active molecule. The active toxin is proposed to bind to cell membrane, leading the membrane pore by toxin oligomerization, and eventually cell becomes lysis (Knowles *et al.*, 1987; Li *et al.*, 1996). Cyt2Aa2 is a cytolytic toxin from *Bacillus thuringiensis* subsp. *darmstadiensis* (*Btd*). It is produced as a 29-kDa protoxin and then proteolytic processed to a 25-kDa activated form in alkali condition. It is specifically toxic against dipteran larvae (*Culex sp, Stegomyia sp*.) *in vivo,* and also active to several cell types such as erythrocytes and fibroblasts (Promdonkoy *et al.*, 2003). Cyt2Aa2 protoxin consists of 259 amino acids that show identical sequence to Cyt2Aa1 from *B. thuringiensis* subsp. *kyushuensis*, both toxins should adopt a similar α/β structure containing 6 α-helices and 7 β-sheets (Koni *et al.*, 1993; Promdonkoy *et al.*, 2004). The β-sheets are located in the interior, wrapped by helices, αA, αB, αC and αD. It was found that the lengths of these helices are not enough to span the membrane and create the pore, whereas the lengths of β-sheets are more suitable (Li *et al.*, 1996). Li et al. (2001) proposed that β5, β6 and β7 which are long enough to span the membrane should insert into the membrane. These sheets from several molecules may oligomerise and form "β-barrel" pore similar to that of α-hemolysin (Song et al., 1996) The possible roles of the helices may involve with binding onto the cell membrane, facilitate the insertion of β-sheets and also the oligomerization of toxin molecules to generate pore (Promdonkoy *et al.*, 2005; 2000). Cyt toxin is structurally related to a few toxins, volvatoxin A2 (VVA) (Lin *et al.*, 2004) and Evf toxin from *Erwinia carotovora*. For Evf toxin, it was found that C209 was involved with pamitate binding site via thioester linkage. This interaction enhanced the strength of toxin

Copyright by Kasetsart University All rights reserved

binding to the membrane (Quevillon-Cheruel *et al.,* 2009). Mapping between Cyt and Evf toxins revealed that the lipid binding cavity of Cyt toxin might locate on alpha C (M110), alpha D (I139), loop between alpha-D and beta-4 at the residues, T142, T144, N145, L146 and beta-7 (V215). Also, the electrostatic surface was identified in Cyt and was proposed that these residues, V150, N159, L160, D209 and T221, were involved with lipid binding pocket (Rigden *et al.,* 2009). Hypothesis for this study is the amino acids in αD, loop between β4 and β5, and β7 of Cyt2Aa2 toxin are involved in membrane binding as well as complex formation. This study attempts to elucidate the role of expected membrane binding residues whether these residues are important for binding and activity of Cyt toxin. The results from this study will reveal more information of membrane binding of Cyt toxin which leads to more understanding of its mechanism.

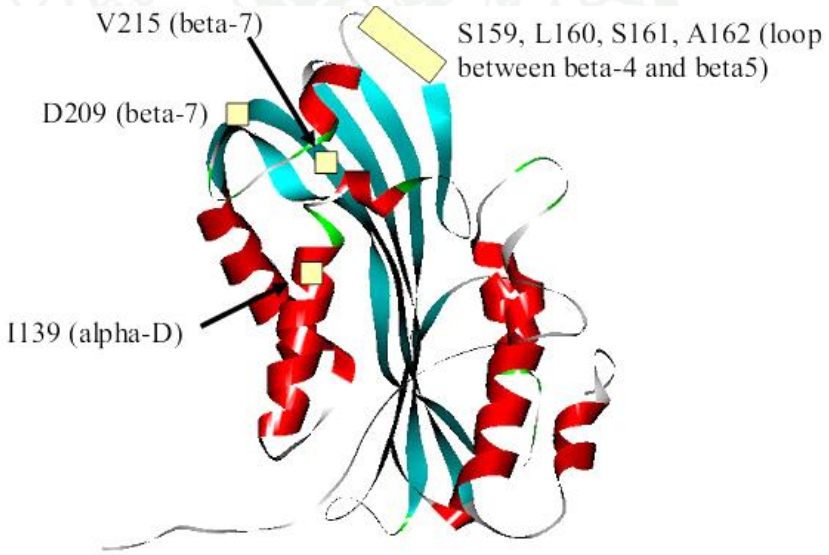

Figure 1 Location of predicted membrane binding residues in Cyt2A toxin.

Copyright by Kasetsart University All rights reserved

OBJECTIVE

To characterize the role of expected lipid binding residues (S159, L160, S161, A162, I139, D209 and V215) whether these residues are important for membrane binding of Cyt toxin.

Copyright by Kasetsart University All rights reserved

LITERATURE REVIEW

1. *Bacillus thuringiensis*

Bacillus thuringiensis (*Bt*) is a gram-positive soil-dwelling bacterium that readily proliferates when environmental conditions such as temperature and nutrient availability are favourable. The formation of spores have been shown to be triggered by internal and external factors including signals for nutrient starvation, cell density and cell cycle progression. The life cycle of *Bt* is characterized by two phases which includs vegetative cell division and spore development, referred as the sporulation cycle (Bulla *et al.,* 1980). The vegetative cell is rod-shaped and divides into two uniform daughter cells by formation of a division septum initiated midway along the plasma membrane. Sporulation, on the other hand, involves asymmetric cell division and is characterized by seven stages (Bechtel *et al.,* 1982) which include (stage I) axial filament formation, (stage II) forespore septum formation, (stage III) engulfment, first appearance of parasporal crystals and formation of a forespore, (stages IV to VI) formation of exosporium, primordial cell wall, cortex and spore coats accompanied by transformation of the spore nucleoid and (stage VII) spore maturation and sporangial lysis.

Bt produces different insecticidal proteins during its sporulation phase of growth. These proteins accumulate as inclusion bodies and are finally released to the environment along with the spore at the end of sporulation. When insects ingest these inclusion bodies, the insecticidal proteins are solubilized in the insect gut juice and they kill the larvae by forming pores in the apical membrane of their midgut cells. These proteins have been used extensively in the control of different insect pests, which are the problems to agricultural crops. These proteins are also active against mosquitoes that are important vectors of human diseases such as malaria and dengue fever. *Bt* produces insecticidal proteins as crystal inclusions composed of two big families Cry and Cyt toxins during sporulation phase of growth (Bravo *et al.,* 2011).

Copyright by Kasetsart University All rights reserved

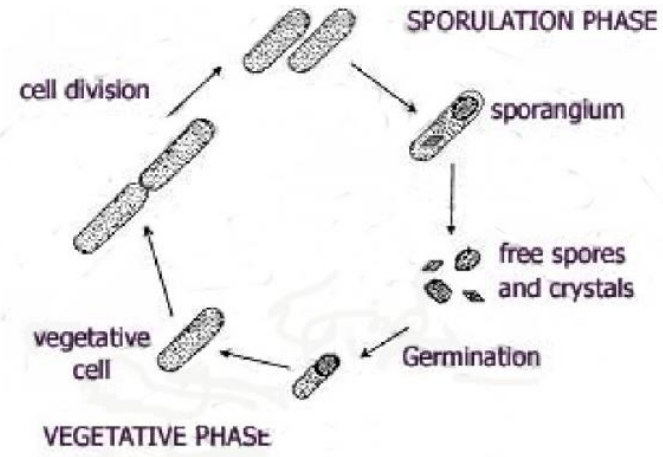

Figure 2 Life cycle of *B. thuringiensis.*

Source: Wuhan (2002)

Bt produce crystal proteins during sporulation that probably, relieves stress physically by offsetting water loss and affords an additional survival advantage by exerting lethal action against host insects. The *Bt* toxin is species-specific and non-pathogenic to humans. However, *Bt* targets pests in the orders Lepidoptera, Coleptera, and Diptera (Thomas *et al.*, 1983).

2. Characteristics of Cytolytic toxin

Cytolytic (Cyt) toxins are a group of proteins produced from some strains of *Bacillus thuringiensis*. These proteins have lethal activity against larvae of dipteran insects *in vivo* and have cytolytic activity against a broad range of cells including erythrocytes *in vitro* (Thomas *et al.*, 1983). To date, a variety of different Cyt toxins have been found in mosquito larvicidal *Bt* strains, and the genes encoding some of these toxins have been identified and sequenced (Ragni *et al.*, 1996).

The insecticidal crystal proteins are produced from *Bt* during sporulation. Amino acid sequences of the crystal proteins can be divided into two major families, Cry and Cyt toxins. These toxins exhibit very high specificity to various insect larvae and some other invertebrates (Schnepf *et al*., 1998). Proteins in the Cry and Cyt

Copyright by Kasetsart University All rights reserved

families have modes of action similarly, although structures of both families are entirely different. The susceptible insect larvae ingested the toxin crystals. These toxin are solubilized in the alkali condition of the insect gut and and become insecticidal after proteolysis by insect gut proteases. The toxin molecules then bind and insert into the epithelial cell membrane that lines the gut lumen, oligomerize, and form pores, leading to osmotic imbalance, cell swelling and osmotic lysis (Knowles and Ellar, 1987).

Bacillus thuringiensis subsp. *darmstadiensis* (*Btd*) is one of the mosquito larvicidal *Bt* strains that can produce both Cry and Cyt toxins. Immunological testing experiments showed that Cyt toxin from Btd 73E10-2 reacted with antibody raised against Cyt2Aa1 but did not react with anti-Cyt1Aa1 (Drobniewski *et al.*, 1989). This result suggested that *Btd* 73E10-2 contains a cyt2A-like gene.

The Cyt δ-endotoxin form a small family of nine known members. They are structurally related to a cardiotoxic pore forming toxin (PFT) called volvatoxin A2, which is produced by the straw mushroom *Volvariella volvacea* (Lin *et al.*, 2004). Cyt toxins have a molecular mass of approximately 25 kDa in their active form (Li *et al.*, 2001). Cyt toxins have a single α-β domain comprising of two outer layers of α-helix hairpins wrapped around by the β-sheets. Cyt toxins are highly specific against the larvae of dipterans, that is mosquitoes and black flies, and they are broadly cytolytic *in vitro*. Cyt toxins can insert into pure liposomal lipid bilayers without any need for a protein co-factor as receptor mediated mechanism for insertion. Like the Cry toxins, Cyt toxins undergo the same steps of solubilization, proteolytic activation and membrane insertion. So far, six Cyt δ-endotoxins have been sequenced and characterized, including Cyt1Aa (previously CytA) and Cyt2Aa (previously CytB). Both Cyt1Aa and Cyt2Aa have been sequenced and characterized by Koni and Ellar. Cyt1Aa has 249 amino acid residues and Cyt2Aa has 259 amino acid residues. They share 39% sequence identity and are expected to be very similar in structure (Koni *et al.*, 1993).

Copyright by Kasetsart University All rights reserved

3. Structure and mechanism of action of Cyt toxins

The structures of three Cyt proteins have been solved, Cyt1Aa, Cyt2Aa and Cyt2Ba showing similar topology displaying a single α-β domain composed of two outer layers of α-helix hairpins wrapped around by the β-sheets. The α-helices have an amphiphilic character, with the hydrophobic residues packed against the β-sheets (Cohen *et al.*, 2008).

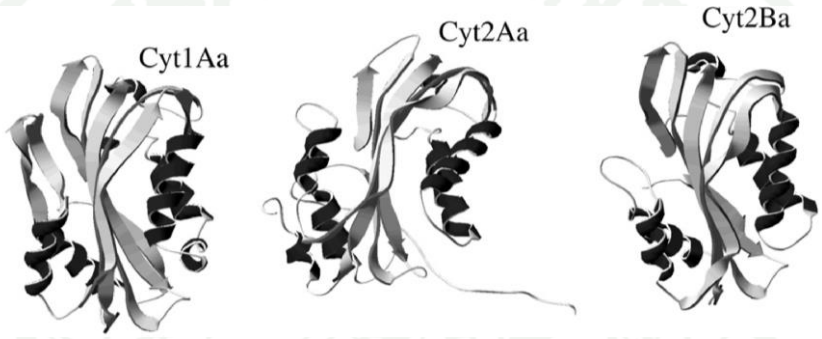

Figure 3 Three-dimensional structure of Cyt toxins from *Bacillus thuringiensis* displayed by Swiss PDB viewer. Cyt1Aa, pdb 3RON; Cyt2Aa, pdb 1CBY; and Cyt2Ba, pdb 2RCI.

Source: Soberon and Bravo (2013)

The activated Cyt toxin is not required midgut proteins for binding with the midgut epithelium. Cyt toxin interact with non-saturated membrane lipids, such as phosphatidylcholine, phosphatidylethanolamine and sphingomyelin and insert into the membrane forming lytic pores (Thomas *et al.*, 1983). Apparently no protein receptors are involved in the mechanism of action of Cyt, which may indicate that interaction with dipteran lipids is quite specific since these proteins are highly specific against dipteran insects *in vivo* and have no effect in other insects (Thomas *et al.*, 1983 and Bravo *et al.*, 2011). The pore formation model proposes that the two outer layers of α -helix hairpins of Cyt toxins swing away from the β -sheet and then the β -strands are able to insert into the membrane forming a β -barrel pore after oligomerization of 16 Cyt subunits (Li *et al*., 1996)

Copyright by Kasetsart University All rights reserved

Two hypotheses in figure 4 have been proposed to explain the membrane insertion of Cyt toxins into dipteran midgut cells. A pore formation model where Cyt toxin binds to the cell membrane, inducing the formation of cation-selective channels in the membrane vesicles leading to colloid-osmotic lysis of the cell (Li *et al.,* 1996; Promdonkoy *et al.*, 2003). Another model is a detergent effect model that proposes a nonspecific aggregation of the toxin on the surface of the lipid bilayer leading to membrane disassembly and cell death (Butko *et al*., 2003).

The α-helices that are present in Cyt toxins are not long enough to span through the membrane bilayer (Li *et al.*, 1996). In contrast, the β-strands 5-7 have an estimated length that could span the width of the biological membrane (Li *et al.*, 1996). The pore formation model proposes that the two outer layers of α-helices hairpins swing away from the β-sheet upon membrane contact, and then the long β-strands are allowed to insert into the membrane. Oligomerization proceeds, ending with the formation of a structured β-barrel pore, within the membrane, that kills the cells by colloid osmotic lysis (Promdonkoy *et al.*, 2000). In the detergent model, it was proposed that Cyt toxins aggregate and are absorbed on the membrane surface causing nonspecific defects in lipid packing, in a similar mechanism to the carpet model formulated for antimicrobial peptides (Shai *et al.*, 1995). In this model, the proteins do not insert into the membrane and may be unstructured. In fact, it was shown that when the Cyt1Aa is bound to lipids, the toxin exhibits a conformation similar to the molten-globule state (Manceva *et al.*, 2004). Thus it was proposed that in the presence of Cyt toxin, the lipids are disordered causing membrane break down into protein-lipid complexes (Manceva *et al.*, 2005). Each can operate at different toxin concentration or on different time scales. While at low concentration the toxin may form oligomeric pores, at high concentrations of the toxin, the membrane may not be able to accommodate the large number of associated molecules and breaks up (Butko *et al.*, 2003).

Copyright by Kasetsart University All rights reserved

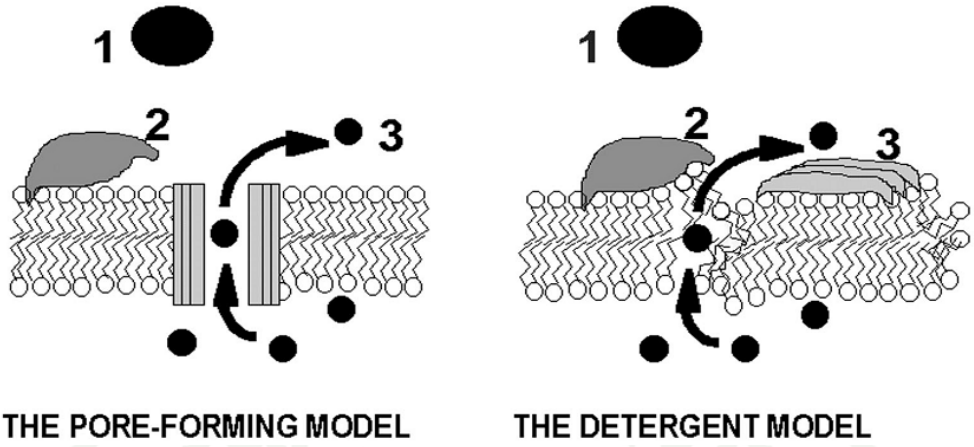

Figure 4 The two hypothetical modes of action of Cyt1A. (1) The soluble toxin (shaded) diffuses in the extracellular phase. (2) During the approach to the membrane, the toxin changes conformation and binds to the lipids. (3) The toxin molecules either insert into the lipid bilayer, where they form oligomeric pores. Intracellular molecules (black circles) leak either through the pores or through introduced lipid packing faults

Source: Butko (2003)

4. Interaction of Cyt toxin with the membrane and pore formation activity

When the Cyt toxin is activated by proteases in solution the toxin remains in its monomeric state as a 25-kDa protein. However, when it is activated in the presence of lipid membrane, it aggregates forming high molecular weight oligomers of 400 kDa (Manceva *et al.*, 2005). The pH may play an important role, since pH induces the destabilization of the tertiary structure of the toxin, and at decreasing pH the Cyt1A surface hydrophobicity increases (Manceva *et al.*, 2003). The binding of Cyt toxin to lipids, may display different apparent association constants at different pH where low pH increases toxin efficiency. The molecular size of aggregate toxins remain constant even at high toxin concentrations, suggesting an ordered oligomerization state of the toxin. It was estimated that the oligomer of Cyt1Aa is composed of 16 monomer molecules based on density gradient centrifugation analysis (Chow *et al.*, 1989).

Copyright by Kasetsart University All rights reserved

In the monomeric structure of Cyt2Aa toxin, the α-helices A, B, C and D are amphipathic, with hydrophobic residues packed against the β-sheets (Li *et al*., 1996). Site directed mutagenesis studies suggested that the region between α-helices A and D may be involved in toxin oligomerization (Promdonkoy *et al.*, 2003). Studies performed with synthetic peptides of Cyt1A, showed that peptides corresponding to α-helices A and C are major structural elements involved in the membrane interaction. These were able to increase the insertion of the Cyt1Aa toxin into the membrane. These regions of the toxin may serve as the structural seeding elements that trigger the oligomerization process of Cyt1Aa (Gazit *et al.*, 1997). In fact, it was shown later that mutations in α-helices A (A61C) and C (S108C) of Cyt2Aa resulted in proteins affected in oligomerization and severely affected in their hemolytic activity, confirming that these α-helices are involved in toxin oligomerization, and that toxin oligomerization is a necessary step for toxin action (Promdonkoy *et al.*, 2007). Finally the N- and C-terminal fragments of Cyt1Aa toxin were cloned, expressed in *Bt* separately, and the functional role of each region was analyzed. The N-terminal region of Cyt1Aa, that comprised the region rich in α-helices, induced toxin aggregation in the absence of lipids. The observed aggregates were similar in size as those found when the Cyt1Aa interacts with membrane lipids (Rodríguez-Almazán *et al.*, 2011). The N-terminal fragment was able to inhibit the hemolytic activity of the toxin *in vitro* and also the *in vivo* insecticidal activity against *A. aegypti* larvae. The observed inhibition of *in vitro* and *in vivo* activity was dominant negative, since sub-stoichiometric mixtures of N-terminal fragment with wild type toxin were able to block the hemolytic activity against red blood cells and the toxicity of Cyt1Aa toxin against *A. aegypti* larvae (Rodríguez-Almazán *et al.*, 2011). These results suggest that the oligomer formation is critical for insecticidal activity of Cyt1Aa, and that the aggregated toxins were formed in solution in the presence of the N-terminal fragment are unable to insert into the membrane.

Cyt1Aa toxin is able to form channels that are slightly selective for monovalent cations. Li et al. proposed that β-strands 5, 6 and 7 inserted into the membrane to form an oligomeric pore with a β-barrel structure. Experiments performed with labeled Cyt2Aa with a fluorescent acrylodan dye, that is highly sensitive to the polar environment, confirmed that these β-strands are inserted into the membrane

Copyright by Kasetsart University All rights reserved

(Promdonkoy *et al.*, 2000). In addition, it was shown that the same β-strands were protected from proteolysis with proteinase K in the membrane-inserted state, supporting that they are buried within hydrophobic environment of the membrane. The membrane-inserted structure retains its pore activity even after proteinase K proteolysis (Du *et al.*, 1999). In relation to these data, it was shown that the purified C-terminal fragment of Cyt1Aa, composed of these three β-strands, inserts into the membrane and retains its capacity to affect the integrity of the membrane as evidenced by its ability to induce calcein release from liposomes (Rodríguez-Almazán *et al.*, 2011). Finally, it is interesting to note that the amino acid sequence of β-strands 5 and 7 show an alternating pattern of hydrophobic and hydrophilic residues, similar to other membrane spanning regions described in different pore forming toxins such as aerolysin, anthrax protective antigen and CDC-toxins (Parker *et al.*, 2005).

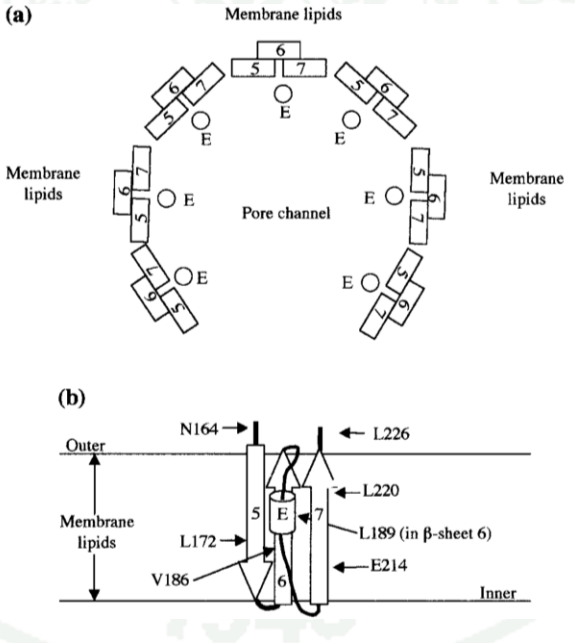

Figure 5 Proposed model for pore structure Top view (a) and side view (b) of a proposed model for pore structure, showing the regions suggested to be inserted in the membrane together with the approximate locations of each of the mutated residues Leu-172, Val-186, Leu-189, Leu-220 and Glu-214. The three b-strands (β5, β6 and β7) are labelled 5, 6 and 7; E denotesa-helix E as described by Li *et al*; 1996. The inner (cytoplasmic) and outer surfaces of the plasma membrane are indicated

Source: Promdonkoy and Ellar (2000)

Copyright by Kasetsart University All rights reserved

5. Similarities of Cyt toxins with other proteins

Figure 6 shows the phylogenetic tree that was performed by maximum likelihood analysis (Guindon *et al.*, 2011). The different Cyt1 toxins from *Bt* are clustered in the same branch with homologous proteins produced by other pathogenic bacteria such as *Aeromonas salmonicida* and *Clostridium kluyveri*. The Cyt2 toxins from *Bt* are clustered with the Cyt-related toxin from *S. venezuelae*. The Cyt-related toxins from *Dickeya zeae* (C6CLD5) and *D. dadantii* (E0SJ35) are highly related and grouped in a separate branch. Similarly other two sequences from *D. dadantii* (E0SJ32 and C6C3H2) are highly related and grouped in a separate branch. Finally the Cyt-related proteins produced by fungus *G. zeae* and *Schizophyllum commune* are the most distant sequences that were found grouped in a separate branch (Soberón *et al*., 2012).

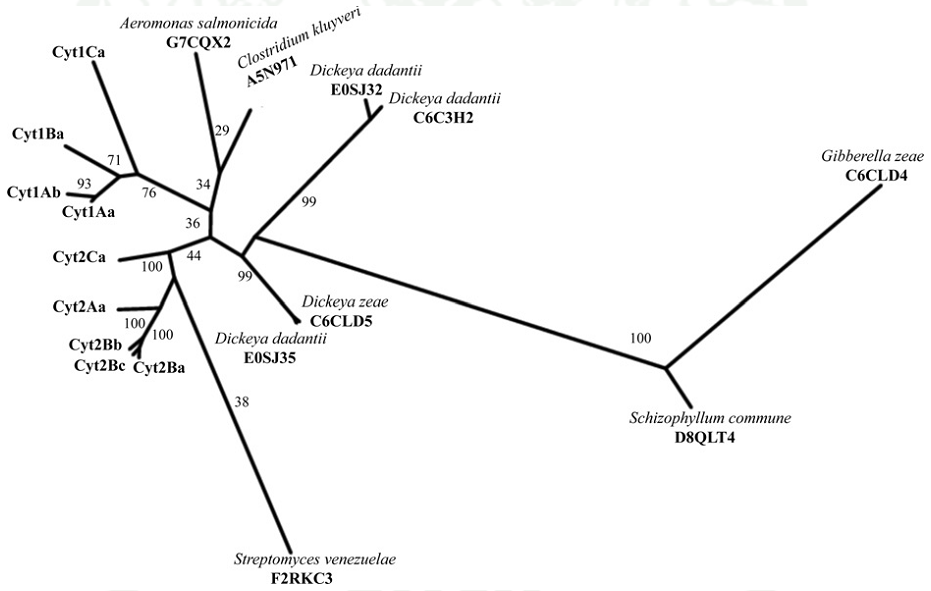

Figure 6 Phylogenetic tree performed by maximum likelihood analysis

Source: Soberón *et al.* (2012)

It was reported that the insect pathogen *Erwinia carotovora* produces a virulence factor named Evf, which showed similar crystal structure to the Cyt2Aa from *Bt* (Quevillon-Cheruel *et al.*, 2009). Also the mushroom *Volvariella volvacea* produced a pore forming cardiotoxin named volvatoxin A2 (VVA2) that shares a

Copyright by Kasetsart University All rights reserved

similar fold to Cyt toxins from *Bt* (Li *et al.*, 2004). Both proteins have low sequence homology with Bt-Cyt toxins. The Evf is related to proteins produced by other bacteria such as *Xenorhabdus bovienii* and *Photorhabdus luminescens* that are nematode-symbiotic pathogens of insects. These two bacteria live in the gut of an entomopathogenic nematode and when the nematode infects an insect, the bacteria are released into the blood stream and rapidly kill the insect, since they produce multiple virulent factors (Manceva *et al.*, 2005).

6. Cyt2Aa2 and other structure related proteins

Biochemical data can be interpreted as favouring a detergent-like model which an initial electrostatic interaction between phospholipid head group and charged toxin residues is followed by an irreversible second step involving hydrophobic and van der Waals forces (Manceva *et al.*, 2005). The structures have allowed mapping of mutations of charged residues (Butko *et al.*, 2003) that significantly affect Cyt toxin activity (Ward *et al.*, 1988) but the location of the binding site that confers the toxin's specificity for unsaturated fatty acids in bound phospholipids remains unidentified (Thomas *et al.*, 1983).

Homologues of Cyt toxins that can be identified by sequence searches in the present databases are confined to volvatoxin and two other potential fungal toxins. However, it is often in the case that distant homology can be recognised at a structural level even when evolution has eroded sequence similarity. The structure of *Erwinia virulence* factor (Evf) has recently been reported to contain a Cys-attached, covalently bound palmitate molecule and have novel topology (Quevillon-Cheruel *et al.*, 2009). Like Cyt proteins, Evf is involved in bacterium–insect interaction, promoting the persistence of *E. carotovora* in the gut of Drosophila larvae, and thereby enhancing bacterial transmission (Basset *et al.*, 2003). Also like Cyt proteins, Evf interacts electrostatically with phospholipids (Quevillon-Cheruel *et al.*, 2009). It is not yet known whether Evf also has specificity for membrane bound lipid. They report that Evf and Cyt proteins in fact share a complex fold indicating shared distant homology. This relationship allows for the identification of a putative fatty acid binding site in Cyt toxins, in good agreement with experimental data (Daniel, 2009)

Copyright by Kasetsart University All rights reserved

The VVA2 and Cyt2Aa1 from *B. thuringiensis sp. kyushuensis* (PDB entry 1CBY) are structural neigbor (Guerchicoff *et al.*, 2001). Activated Cyt toxins and VVA2 share similar comparable sequence lengths. However, the protein sequence identity between VVA2 and Cyt2Aa1 is low (19.6% over the 194 amino acid residues, Figure 8. The Cyt2Aa1 structure was resolved in the inactive protoxin form contains a single α/β domain, which comprises of a three-layered core, with a six-stranded β-sheet flanked by two helix hairpins, and cleavable extensions at both N-terminal and C-terminal ends (Li *et al*., 1996). Cyt2Aa1 is a dimer linked by the intertwined N-terminal extension (Li *et al*., 1996). The arrangement of the β strands and α helices of the Cyt2Aa1 monomer structure, which represents a unique cytolysin fold, resembles the structure of VVA2, except that the β-hairpin inserted in the loop αA-αB region of VVA2 is absent from Cyt2Aa1 and αD shifts a little (Figure 8). Nevertheless, the VVA2 structures presented here were solved in the active toxin form and could provide structural information about activated toxins. Differences between VVA2 and Cyt2Aa1center on $loop_{\beta2\text{-}\beta3}$, $loop_{\alpha B\text{-}\beta4}$, $loop_{\alpha C\text{-}\alpha D}$, $loop_{\beta5\text{-}\beta6}$, and $loop_{\beta6\text{-}\beta7}$ (Figure 7). The N-terminal and C-terminal extensions of Cyt2Aa1 would result in significant steric hindrance. Proteolytic processing at both N-terminal and C-terminal extensions could make Cyt2Aa1 adopt an “active” conformation similar to VVA2 and allow transient oligomerization of Cyt2Aa1 through the region corresponding to the residues Ala91 to Ala101 of VVA2. Notably, there are only 18 conserved residues (9.3% of total residues) between VVA2 and Cyt toxins (Figure 7). VVA2 is the first active form structure with the cytolysin fold previously observed in Cyt2Aa1 (Lin *et al*., 2004).

Copyright by Kasetsart University All rights reserved

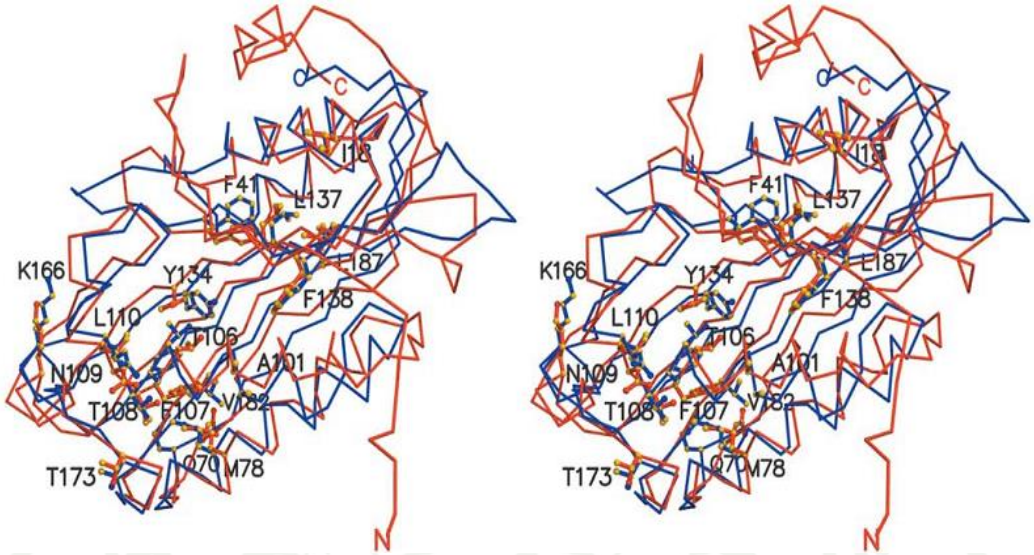

Figure 7 Comparison of the structures between VVA2 and Cyt. Stereo C^{α} trace of the superimposed VVA2 and Cyt2Aa1. VVA2 and Cyt2Aa1 are shown in blue and red, respectively. The absolutely conserved residues are shown as ball-and-sticks.

Source: Lin *et al*. (2004)

Copyright by Kasetsart University All rights reserved

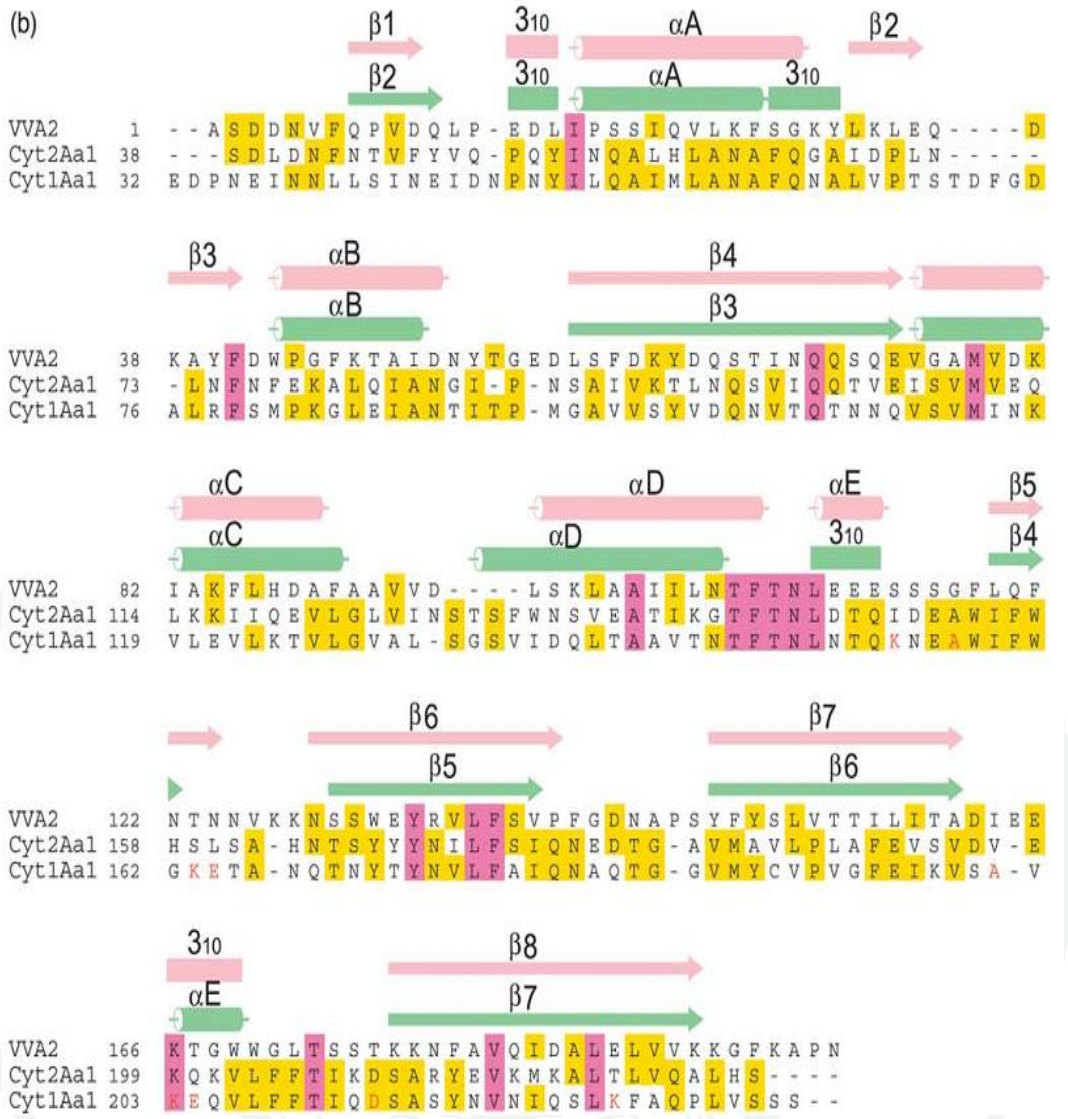

Figure 8 Comparison of the sequences between VVA2 and Cyt. Alignment of sequences of VVA2 with Cyt2Aa1 and Cyt1Aa1 from *B. thuringiensis*. Secondary structural elements of VVA2 and Cyt2Aa1 are shown in pink and green, respectively. Conservative residues are masked in crimson (absolutely conserved) or yellow. The red residues indicate low-toxicity mutations in Cyt1Aa1. The sequences of Cyt toxins after proteolytic activation are shown.

Source: Lin *et al*. (2004)

Copyright by Kasetsart University All rights reserved

Due to the structural similarity between VVA2 and Cyt2Aa1, it seems plausible that VVA2 and Cyt2Aa1 could have similar pore-forming mechanisms and adopt similar molecular packing to form a pore. Proteolytic analyses have shown that the membrane-protected fragment of Cyt2Aa1 corresponds to that of VVA2 (Weng *et al*., 2004). This fragment contains three long β-strands (corresponding to β6, β7 and β8 in VVA2), which were proposed to enter the lipid bilayer (Promdonkoy *et al*., 2000) The amphipathic character of these three β-strands was thought to be important for Cyt2Aa1's pore formation (Li *et al*., 2001). On β-strands, β6, β7 and β8 in VVA2, 13 out of 21 residues facing αCD- hairpin are hydrophobic, while eight out of 20 residues facing α/β-hairpin are hydrophobic. This shows that three long β-strands in VVA2, β 6, β 7and β 8, also have amphipathic character similar to that of the corresponding β-strands of Cyt2Aa1. This suggests that β6, β7and β8 would play an important role in VVA2's pore formation. It has been proposed that the pore of Cyt2Aa1 consists of four, five, or six subunits, and each subunit donates three β-strands (Promdonkoy *et al*., 2000).

In VVA2, the proposed pore contains 18 subunits with 9-fold symmetry. If each of the VVA2 subunits in layer AB donated two β-strands (e.g. β6 and β7) for the assembly of an 18 stranded β-barrel, VVA2 could form a transmembrane pore of similar size and pore structure with a molecular mass comparable to that of Cyt2Aa1. The pore model of VVA2 proposed fits the experimental data of Cyt toxin from *B. thuringiensis* (Lin *et al*., 2004).

7. Evf and cytolytic toxins share a fold

The crystal of Evf was reported its topology that based on structural comparisons carried out using solely the secondary-structure matching (SSM) method (Krissinel and Henrick, 2004). Comparisons of structure similarity search algorithms consistently showed wide, case-specific variation (Zhu and Weng, 2005) leading to the recommendation that such searches employ several methods and seek a consensus between them (Novotny *et al.*, 2004)

Copyright by Kasetsart University All rights reserved

Using the DALI and FATCAT methods for structural alignment of proteins revealed significant structural similarity between Evf (PDB code 2w3y) (Quevillon-Cheruel *et al*., 2009) and the structures of Cyt2Aa (PDB code 1cby) and Cyt2Ba (PDB code 2rci) as well as the structure of the homologous fungal toxin volvatoxin (several PDB codes). Figure 9 shows a comparison of Evf and Cyt2Ba structures, Evf and the cytolytic toxins share all of the major components of the fold. Start of core fold to end were coloured blue and red, respectively. In both cases a five-stranded β-sheet is flanked on both sides by helices. The unique terminal regions of Evf shown in grey form additional helices and its palmitoyl-cysteine residue in stick representation, toward the C-terminus, an additional, sixth strand to the β-sheet. The structurally different regions preceding strand β4 in the two structures are coloured pink. The Evf structure shares the structural of the cytolytic toxin fold. The central β-sheet of Evf has a much greater twist than that of the cytolytic toxins (Figure 9). Sequence identity between Evf and cytolytic toxins were only 6-11% (Murzin, 1993).

Figure 10 shows that even within the two groups, Evf and all homologues (above) and homologues of cytotoxins (below), there is limited sequence identity. Between the two groups there is very little sequence conservation, despite their clearly homology. From analysis of conservation between cytolytic toxin and volvatoxin structures (Cohen *et al.*, 2008) the obvious feature of the toxins is a TFTNL motif at residues 142-146 in Cyt2Ba. By the structural alignment, Evf and relatives conserved the Phe residue and it is often preceded by a Thr or Ser. In the Cyt2Ba, these residues are between helices α4 and η3. In the Evf structure these residues are part of a helix, might form in the fatty acid bound form, may be related with the role of the conformational transition between bound and unbound forms.

The functional relativity between Evf and cytolytic toxins (bacterium-insect interaction, membrane binding) provided support for a distant homology between the two proteins. The most striking feature of the Evf structure, the Cys-bound palmitate, involved with molecular functions of the toxins. (Hamilton., 2004).

Copyright by Kasetsart University All rights reserved

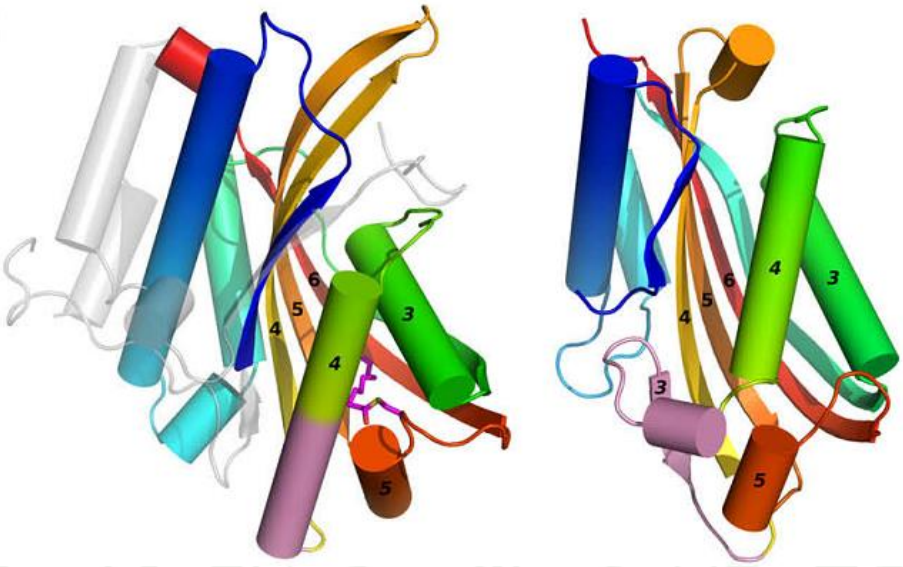

Figure 9 Structural superposition of Evf (Quevillon-Cheruel *et al*., 2009) and Cyt2Ba (Cohen *et al*., 2008) produced by the FATCAT algorithm (Ye and Godzik., 2003) operating in rigid mode. Cartoon representations of Evf (left) and Cyt2Ba (right) coloured from blue (start of core fold) to red (end). Terminal extensions of Evf are shown as semi-transparent grey and its palmitoyl-cysteine residue in stick representation. The structurally different regions preceding strand β4 in the two structures are coloured pink. Secondary structure elements mentioned in the text are labelled using italics for a-helices and normal text forb-strands This figure was produced using PyMOL (DeLano, 2002).

Source: Rigden (2009)

Copyright by Kasetsart University All rights reserved

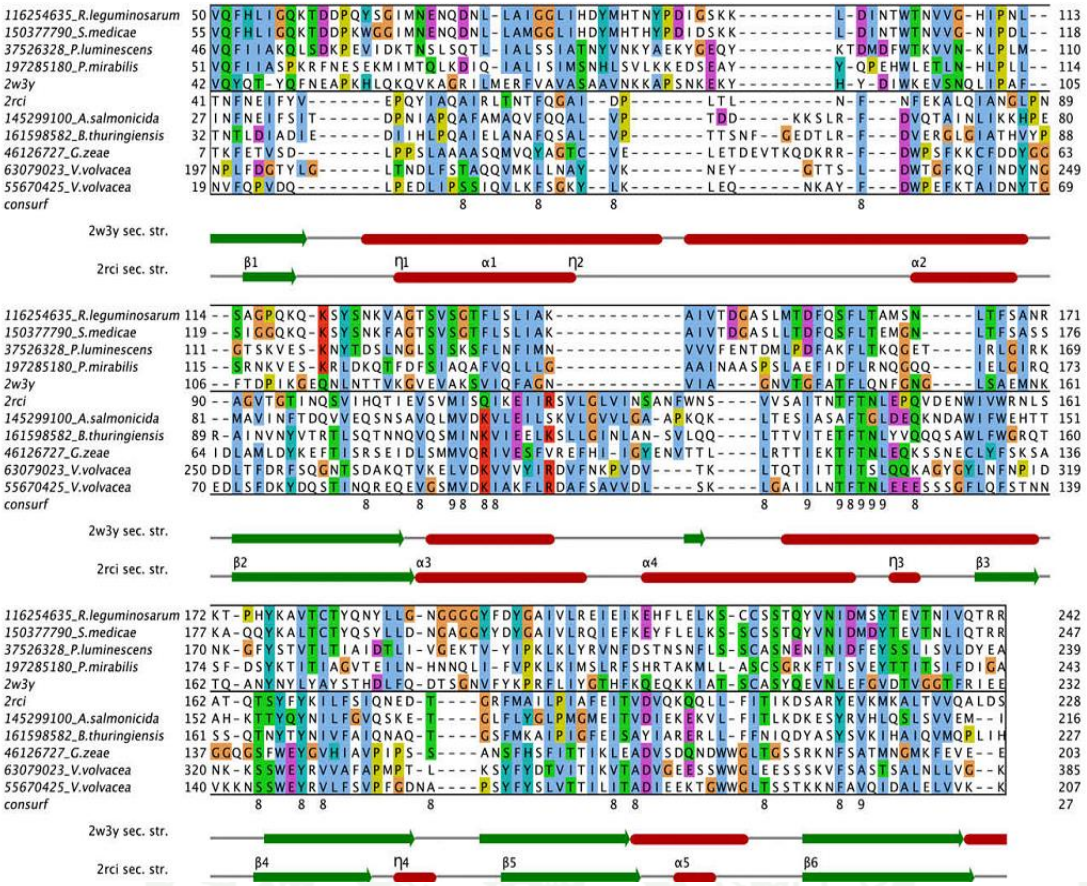

Figure 10 The corresponding structure-based sequence alignment of Evf (Quevillon-Cheruel *et al*., 2009) and Cyt2Ba (Cohen *et al*., 2008). The upper group contains Evf and the four presently available homologous sequences. The lower group contains a redundancy minimised set of representatives of the toxin family. Sequences are labelled with gi number (Wheeler *et al.*, 2007) and species name. Immediately below, numbers 8 and 9 indicate the most conserved positions determined using Consurf (Landau *et al*., 2005) in a complete alignment of the toxin family. Secondary structures are annotated underneath the alignment using the numbering of Cyt2Ba (Cohen *et al*., 2008). Labels η1 onwards refer to 3_{10}helices. This figure was made with Jalview (Clamp *et al*., 2004), which was also used for redundancy removal.

Source: Rigden (2009)

Copyright by Kasetsart University All rights reserved

MATERIALS AND METHODS

Materials

1. Samples and laboratory animals
   1.1 *Aedes aegypti* larvae
   1.2 Hamster
   1.3 Rat red blood cells

2. Chemical agents and kits
   2.1 Acetic acid (AnalaR Normapur®, VWR, U.S.A.)
   2.2 AEC Chromogen Kit (Sigma, USA)
   2.3 Agarose (Vivantis, Malaysia)
   2.4 Ammonium persulfate (APS) (Bio-Rad Laboratories, U.S.A.)
   2.5 Bio-Rad Protein Assay Dye Reagent Concentrate (Bio-Rad Laboratories, U.S.A.)
   2.6 Bovine serum albumin (New England Biolabs, U.S.A.)
   2.7 Coomassie® Brillant Blue R 250 (Fluka)
   2.8 Dimethyl sulfoxide (DMSO) (Vivantis, Malaysia)
   2.9 Deoxyribonucleotide triphosphate (dNTP) (Vivantis, Malaysia)
   2.10 DNA Ladder (1 kb) (New England Biolabs, U.S.A.)
   2.11 Ethanol (AnalaR Normapur®, VWR, U.S.A.)
   2.12 Ethidium bromide (EtBr) (Fluka, Sigma-Aldrich, U.S.A.)
   2.13 FavorPrep™ Gel/PCR Purification Mini Kit (Favorgen, Taiwan)
      a. Collection tube
      b. FADF buffer
      c. FADF column
      d. Elution buffer
      e. Wash Buffer
   2.14 Gel Loading Dye, Blue (6X) (New England Biolabs, U.S.A.)
   2.15 Hydrochloric acid (HCl) (Merck, Germany)
   2.16 Isopropyl alcohol (Merck, Germany)

Copyright by Kasetsart University All rights reserved

2.17 Phenylmethyl Sulfonyl Fluoride (PMSF) (USA Corporation, USA)

2.18 Phusion Hot Start II High-Fidelity DNA Polymerase (Thermo Scientific, U.S.A.)

a. Phusion HF buffer (5x)

b. Phusion Hot Start II High-Fidelity DNA Polymerase

2.19 Sodium chloride (NaCl) (Vivantis, Malaysia)

2.20 Sterile distilled water (SDW)

2.21 Tris(hydroxymethyl)aminomethane (Tris) (Vivantis, Malaysia)

3. Tools

3.1 24-well plate (1.5 cm well diameter) (Thermo Scientific, U.S.A.)

3.2 96-well standard microplate (Thermo Scientific, U.S.A.)

3.3 Absorbent cotton

3.4 Hamster-fitting cage for mosquito feeding

3.5 Microcentrifuge tubes

3.6 Micropipette

3.7 Micropipette tips

3.8 Mosquito cage

3.9 Mosquito sucking tube

3.10 Plastic Pasteur pipette

3.11 Polymerase chain reaction (PCR) tube

3.12 Water tray

4. Machines

4.1 AccuBlock™ Digital Dry Bath (BioExpress Online, U.S.A.)

4.2 Benchtop Centrifuge Sigma 3-18K (Sartorius, U.K.)

4.3 Docu-pH+ meter (Sartorius, U.K.)

4.4 DTX 880 Multimode Detector (Beckman Coulter, U.S.A.)

4.5 Freezer -20°C (Sanyo, Japan)

4.6 Freezer -80°C (Forma scientific, U.S.A.)

4.7 G-Storm GS482 Thermal Cycler (Labtech, U.K.)

4.8 Hot air oven (Memmert GmbH +, Germany)

Copyright by Kasetsart University All rights reserved

4.9 Icemaker (Newton Equipment, Thailand)

4.10 Mini Horizontal Gel Electrophoresis System (Major Science, U.S.A.)

4.11 Gel electrophoresis chamber

4.12 Gel tray and stand

4.13 Well comb

4.14 Molecular Imager® Gel Doc™ XR+ System (Bio-Rad Laboratories, U.S.A.)

4.15 NanoDrop 2000 UV-Vis Spectrophotometers (Thermo Scientific, U.S.A.)

4.16 PowerPac™ Basic Power Supply (Bio-Rad Laboratories, U.S.A.)

4.17 Refrigerator (Sanyo, Japan)

4.18 Spectroline® Ultraviolet transilluminator (Spectronics, U.S.A.)

4.19 Tomy SX-700 High-Pressure Steam Sterilizer (Tomy Digital Biology, Japan)

5. Computer programs, online database and tools

5.1 Basic Local Alignment Search Tool (BLAST) (Camacho *et al.*, 2008)

5.2 ClustalW2 (Larkin *et al.*, 2007)

5.3 ExPASy Translate tool (Swiss Institute of Bioinformatics, Switzerland)

5.4 GenBank (Benson *et al*., 2013)

5.5 Microsoft Excel 2010 (Microsoft, U.S.A.)

5.6 NanoDrop 2000 / 2000c Software (Thermo Scientific, U.S.A.)

5.7 StatPlus Professional (Analystsoft, New York version 2008)

Copyright by Kasetsart University All rights reserved

Methods

1. Preparation starting culture for plasmid extraction

The *Escherichia coli* JM109 were used throughout the experiment. The recombinant plasmid pGEM-Cyt2Aa2 (Promdonkoy *et al*., 2003), containing the full-length *cyt2Aa2* gene in the pGEM-T easy vector (Promega) was used. *E. coli* harboring *cyt2Aa2* wild type cell was provided from B. Promdonkoy (National Center for Genetic Engineering and Biotechnology, Thailand). *E. coli* was used as a starting culture for plasmid extraction. The 1-3% of culture was transferred into a new 10 ml of LB broth containing 100 µg/ml ampicillin and grown at 37^{o}C with shaking at 220 rpm for 16-18 hours.

2. Plasmid extraction

The plasmid was extracted by FavorPrep®Plasmid DNA Extraction Kit. The 3 ml of overnight culture were transferred to a microcentrifuge tube. The bacteria was descended by centrifuging for 1 minute at 12,000 rpm and discarded the supernatant completely. The 200 µl of FAPD1 buffer (RNase A added) was added to the pellet and resuspended the cells completely by pipetting. Two hundreds µl of FAPD2 buffer was added and gently inverted the tube 10 times to lyse the cells and incubated at room temperature for 2 minutes. Do not vortex, vortex may shear genomic DNA. Do not proceed this step over 5 minutes. Three hundreds µl of FAPD3 buffer was added and inverted the tube 10 times immediately but gently, and centrifuged for 5 min at full speed. During centrifuging, placed a FAPD column in a collection tube. The supernatant was transferred carefully to FAPD column, and centrifuged for 30 seconds then discarded the flowthrough and placed the FAPD column back in the collection Tube. Four hundreds µl of W1 buffer was added to FAPD column, and centrifuged for 30 seconds then discarded the flowthrough and placed the FAPD column back in the collection Tube. Six hundreds µl of wash buffer (ethanol added) was added to FAPD column, and centrifuged for 30 seconds then discarded the flowthrough and placed the FAPD column back in the collection tube then centrifuged again for an additional 3

Copyright by Kasetsart University All rights reserved

minutes to dry the column. The FAPD column was placed to a new 1.5 ml microcentrifuge. Fifty µl of elution buffer was added to the membrane center of FAPD column, and stood the column for 2 minutes then centrifuged for 1 min to elute plasmid DNA. The plasmid DNA was stored at -20 °C. The plasmid was detected by gel electrophoresis using 0.8% agarose gels comparable to 1 kb of DNA ladder as a marker.

3. Mutagenic primer design

The full-length cyt2Aa2 gene in the pGEM-Teasy vector (Promega) was used as DNA template. Oligonucleotide primers for site directed mutagenesis were obtained from sequences of cyt2Aa2. GenBank accession number for cyt2Aa2 is AF472606. DNA sequences of forward and reverse primers for Cyt2Aa2-mutants are shown in Table 1.

Copyright by Kasetsart University All rights reserved

```
atgtatactaaaaattttagtaattccagaatggaagtaaaaggtaataacgggtgttct
 M  Y  T  K  N  F  S  N  S  R  M  E  V  K  G  N  N  G  C  S
gcacctattattagaaaaccatttaaacatattgtattaacggttccatccagtgattta
 A  P  I  I  R  K  P  F  K  H  I  V  L  T  V  P  S  S  D  L
gataattttaatacagtcttttatgtacaaccacaatacattaatcaggctcttcattta
 D  N  F  N  T  V  F  Y  V  Q  P  Q  Y  I  N  Q  A  L  H  L
gcaaatgcttttcaaggggctatagacccacttaatttaaatttcaattttgaaaaggca
 A  N  A  F  Q  G  A  I  D  P  L  N  L  N  F  N  F  E  K  A
ctccaaattgcaaatggtattcctaattctgcaattgtaaaaactcttaatcaaagtgtt
 L  Q  I  A  N  G  I  P  N  S  A  I  V  K  T  L  N  Q  S  V
atacagcaaacagttgaaatttcagttatggttgagcaacttaaaaagattattcaagag
 I  Q  Q  T  V  E  I  S  V  M  V  E  Q  L  K  K  I  I  Q  E
gttttaggacttgttattaacagtactagtttttggaattcggtagaagctacaattaaa
 V  L  G  L  V  I  N  S  T  S  F  W  N  S  V  E  A  T  I  K
ggcacatttacaaatttagacactcaaatagatgaagcatggatttttttggcatagttta
 G  T  F  T  N  L  D  T  Q  I  D  E  A  W  I  F  W  H  S  L
tccgcccacaatacaagttattattataatattttatttctattcaaaatgaagataca
 S  A  H  N  T  S  Y  Y  Y  N  I  L  F  S  I  Q  N  E  D  T
ggtgcagttatggcagtattacctttagcatttgaggtttctgtggatgttgaaaaacaa
 G  A  V  M  A  V  L  P  L  A  F  E  V  S  V  D  V  E  K  Q
aaagtattattctttacaataaaagatagtgcacgatatgaagttaaaatgaaagctttg
 K  V  L  F  F  T  I  K  D  S  A  R  Y  E  V  K  M  K  A  L
actttagttcaagctctacattcctctaatgccccaattgtagatatatttaatgttaat
 T  L  V  Q  A  L  H  S  S  N  A  P  I  V  D  I  F  N  V  N
aactataatttataccattctaatcataagattattcaaaatttaaatttatcgaattga
 N  Y  N  L  Y  H  S  N  H  K  I  I  Q  N  L  N  L  S  N  -
```

Figure 11 Nucleotide and deduced amino acid sequences of cyt2Aa2. GenBank accession number for cyt2Aa2 is AF472606 (Promdonkoy *et al*., 2003).

Copyright by Kasetsart University All rights reserved

Oligonucleotide primers for site-directed mutagenesis were from Bio Basic Inc. The primer sequences and additional information are shown in Table 1. Primers were designed based on cyt2Aa2gene (GenBank Accession No. AF472606). Mutated nucleotides were underlined. This table showed the forward and reverse primers.

Table 1 Mutagenic primers for site-directed mutagenesis

Primer	Sequence (5'→ 3')
I139AF	5' GAAGCTACAGCTAAAGGCACATTTAC 3'
I139AR	5' GTAAATGTGCCTTTAGCTGTAGCTTC 3'
S159AF	5' GGATTTTTTGGCATGCTTTATCCGCCC 3'
S159AR	5' GGGCGGATAAAGCATGCCAAAAAATCC 3'
L160AF	5' GGCATAGTGCATCCGCCCACAATACAA 3'
L160AR	5' TTGTATTGTGGGCGGATGCACTATGCC 3'
S161AF	5' GGCATAGTTTAGCCGCCCACAATACAAG 3'
S161AR	5' GTTGTATTGTGGGCGGCTAAACTATGCC 3'
A162VF	5' GGCATAGTTTATCCGTACACAATACAAG 3'
A162VR	5' CTTGTATTGTGTACGGATAAACTATGCC 3'
D209NF	5' CAATAAAAAATAGTGCACGATATGAAG 3'
D209NR	5' CTTCATATCGTGCACTATTTTTTATTG 3'
V215AF	5' GTGCACGATATGAAGCTAAAATGAAAGC 3'
V215AR	5' GCTTTCATTTTAGCTTCATATCGTGCAC 3'

4. Mutant construction

4.1 Site-directed mutagenesis

Site-directed mutagenesis, the method used in this work was based on Stratagene's Quik Change Site-Directed Mutagenesis. The recombinant plasmid pGEM-cyt2Aa2 was used as a template for single substitutions I139A, S159A, L160A, S161A, A162V, D209N and V215A together with primers described in Table 1. The

Copyright by Kasetsart University All rights reserved

isoleucine residue at 139 located on alpha-D was changed to alanine. S159, L160, S161 locate on loop between beta-4 and beta5 were changed to alanine except A162 was changed to valine. Aspartate residue at 209 locate on beta-7 was changed to asparagine. Valine residue at 215 locate on beta-7 was changed to alanine.

Following the PCR reaction, 100 ng of the recombinant plasmid pGEM-cyt2Aa2 was mixed with 10 µl of 5x Phusion HF Buffer, 2.5 µl of 50 µM dNTPs, 2 µl of 10 µM forward primer, 2 µl of 10 µM reverse primer, 0.5 µl of 2 units/µl Phusion High-Fidelity DNA Polymerase (Thermo Scientific, U.S.A.) in PCR tube and sterile distilled water was added to make the total volume reched 50 µl. The reaction mixture was incubated at an initial denaturation at 95°C for 1 minute, the 25 cycles of denaturation at 95°C for 30 seconds, annealing at 55°C for 30 seconds, extension at 72°C for 3 minutes and the final extension at 72°C for 5 minutes. PCR products were detected by gel electrophoresis of 0.8% agarose gels. The product is digested with 1 µl DpnI (10 unit) per each PCR reaction and incubated at 37^{o}C for 3 hours and detected by gel electrophoresis of 0.8% agarose gels before transformation. DNA sequences of the full-length *cyt2Aa2 gene* from all mutants were verified by DNA sequencing.

4.2 Preparation of *E. coli* competent cells using $CaCl_2$

E.coli cells were streaked on an LB plate. The cells were grown at 37^{o}C overnight. one colony was placed in 3 ml LB media, grown overnight at 37^{o}C. The 1 ml overnight culture was transferred into 150 ml LB media in 250 ml flask. The cells were grown at 37^{o}C (250 rpm), until OD_{600}= 0.4 (~2-3 hours). The cells were transferred to centrifuge bottles (50 ml), and placed the cells on ice for 30 minutes. The cells were centrifuged at 4^{o}C for 10 minutes at 6,000 rpm. The media was poured off. The cells were resuspended in 10 ml of cold 0.1 M $CaCl_2$, and incubated on ice for 30 minutes. The cells were centrifuged at 4^{o}C for 10 minutes at 6,000 rpm. The supernatant was poured then resuspended cells (by pipetting) in 2 ml cold 0.1 M $CaCl_2$, and placed cells on ice for 5 minutes. Nine hundreds µl of glycerol was added and aliquoted 200 µl into microcentrifuge tube placed on ice. The cells were stored at -80^{o}C .

Copyright by Kasetsart University All rights reserved

4.3 Transformation using heat shock method

The *E. coli* competent cells were taken from -80^{o}C freezer. A 100 ng of the recombinant plasmid pGEM-Cyt2Aa2 mutant was added and mixed with 200 µl of competent cells in a 1.5 ml tube. The tubes were kept on ice for 30 minutes then put into water bath at 42^{o}C for 90 seconds and put tubes back on ice for 5 minutes. The cells were added with 1 ml of LB (with no antibiotic added), incubated for 1 hour at 37^{o}C, and centrifuged for 5 minutes at 3,000 rpm. The media was poured off and remained to 200 µl, and then the resulting culture was spread on LB plates with 100 µg/ml ampicillin added and grown overnight.Three colonies of each mutants were picked and grown in 3 ml LB with 100 µg/ml ampicillin added and incubated at 37^{o}C overnight for plasmid extraction. The plasmid was detected by gel electrophoresis of 0.8% agarose gels. DNA sequencing was performed to confirm mutant DNA sequence.

5. Protein expression

5.1 Small scale protein expression

The colonies of WT and mutants were picked and grown in 3 ml LB with 100 µg/ml ampicillin added and incubated at 37^{o}C overnight. The 1-3% of culture was transferred into a new 50 ml of LB broth containing 100 µg/ml ampicillin. Allow cell to grow at 37^{o}C with shaking at 220 rpm, until OD_{600}= 0.4 (~2-3 hours) then added 0.1 mM IPTG (isopropyl-b-D-thiogalactopyranoside) to grow at 37^{o}C with shaking at 220 rpm for 4 hours. The cells were kept at OD_{600}= 0.5 and transferred to 1.5 ml tubes, centrifuged at 5,000 rpm for 2 minutes. The supernatant was removed, the pellets were resuspened with 50µl sterile water then 4X sample buffer was added and boiled for 5 minutes. Eight µl of sample was subjected in polyacrylamide gel electrophoresis (SDS-PAGE). Total protein was separated on SDS-PAGE and visualized by Coomassie brilliant blue stain R-250.

Copyright by Kasetsart University All rights reserved

5.2 Large scale protein expression

The colonies of WT and mutants were grown in 3ml LB with 100 µg/ml ampicillin added and incubated at 37°C overnight. The 1-3% of culture was transferred into a new 250 ml of LB broth containing 100 µg/ml ampicillin in 500 ml flask. Allow cell to grow at 37°C with shaking at 220 rpm, until OD_{600}= 0.4 (~2-3 hours). One mM IPTG was added to induce the protein expression, incubated at 37°C with shaking at 220 rpm for 5 hours. The cells were transferred to 50 ml tubes, centrifuged at 6,000 rpm for 10 minutes. The supernatant was removed, resuspened the pellets with 20 ml sterile water and kept the tubes on ice. The cells were lysed by an ultrasonicator at 40% amplitude, pulse on 10 seconds and off 5 seconds for 20 minutes in ice. The lysed cell was transferred into 50 ml polypropylene falcon tubes and centrifuged at 12,000 rpm for 10 minutes. The pellet was resuspened in Tris-KCl buffer pH 7.5 for re-sonication at 40% amplitude, pulse on 10 seconds and off 5 seconds for 20 minutes in ice and centrifuged at 12,000 rpm for 10 minutes, then washed with 10 ml Tris-KCl buffer pH 7.5 for 3 times. The pellet was resuspened with 3 ml sterile water as inclusion bodies. The inclusion bodies were stored at -20°C. The lysed cell, soluble fractions and inclusion bodies of all mutant and wild type were analyzed on 12% SDS-PAGE.

6. Solubilization and activation of Cyt2Aa2

The inclusion bodies was solubilized in 50 mM bicarbonate buffer (Na_2CO_3/$NaHCO_3$) pH 10.5 at the ratio 1:1 inclusion to the buffer, incubated at 37 °C for 1 hour. The supernatant was collected by centrifugation at 12000 rpm for 10 minutes. The protoxin of Cyt2Aa2 and mutants were digested by proteinase K at the ratio 100:1 toxin to proteinase K, incubated at 37 °C for 1 hour. The activity of proteinase K was inhibited by 4 mM phenylmethanesul- fonylfluoride (PMSF). The solubility of protoxins and the activated toxins were analyzed on 12% SDS-PAGE.

Copyright by Kasetsart University All rights reserved

7. *Aedes aegypti* cultivation

The eggs of *A. aegypti* was incubated in a cup of water at room temperature until they were hatched. A level of water was maintained to cover all of the eggs. The larvae were transferred into water tray by plastic pasteur pipette. The larvae were fed with 10-30 mg of fish food depend on their sizes one time a day. The water in a tray was changed every 2-3 days. The pupae were transferred to a cup of water in a box that covered with mosquito net. The adult mosquitoes would moulted from the pupae in 1-3 days. The adult mosquitoes were left in the box for 3-5 days to breed at 25°C. The syrup-soaked absorbent cotton was placed on the mosquito net to feed mosquitoes. A hamster was captured in a cage that fitted to its body. The hamster in a cage was then put in a mosquito cage for 20 minutes for blood feeding. Two days after blood feeding, a cup of paper with water was provided into the mosquito cage for egg laying. The *A. aegypti* cultivation place and materials was provided by Laboratory of Prof. Theeraphap Chareonviriyaphap, Department of Entomology, Faculty of Agriculture, Kasetsart University.

8. Mosquito-larvicidal assay

The 3rd instar *A. aegypti* larvae were fed with two-fold serial dilutions of toxin inclusions from 0.12 to 250 µg/ml diluted in distilled water. One ml of the serial diluted inclusion was added to a 24-well plate (1.5 cm well diameter) containing 10 larvae in 1 ml of distilled water. The mortality was recorded after 24 hours of incubation at room temperature and LC_{50} value (concentration of toxin that caused 50% mortality) was determined by Probit analysis.

9. Preparation of 2% rat red blood cells in PBS buffer pH 7.4

One ml of the rat red blood cells (RBC) in 1.5 ml tube was centrifuged at 4^{o}C, 3,000g for 5 minutes. The supernatant was removed, the RBC was washed with 1 ml PBS buffer (8 mM Na_2HPO_4,1.5 mM KH_2PO_4, 140 mM NaCl, 2.7 mM KCl, pH 7.4) and centrifuged at 4^{o}C, 3,000g for 5 minutes, washed until the supernatant was clear,

Copyright by Kasetsart University All rights reserved

then remove supernatant. A suspension of 2% (v/v) red blood cells was prepared in PBS buffer.

10. Hemolysis assay

A suspension of 2% RBC was prepared in PBS buffer. Hemolytic assay was performed by adding the two-fold serial dilutions of the activated Cyt2Aa2 wild type or its mutants in PBS pH 7.4 in a 96-well microtiter plate. One hundred µl of the serial diluted toxin (0.024-50 µg/ml) was mixed with 100 µl of 2% RBC. The hemolytic endpoint was monitored after 24 hours of incubation at room temperature.

11. Hemoglobin release assay

Hemoglobin release assay was performed using the method previously described (Promdonkoy and Ellar, 2003). One hundred µl of 2% rat RBCs in PBS pH 7.4 were incubated with various concentrations of 100 µl activated toxins (0.5–12 µg/ml) for 2 hours at room temperature. Unbroken cells and cell debris were removed by centrifugation at 12,000g for 30 seconds. Hemoglobin in supernatant was determined by measuring absorbance at 540 nm using ELISA plate reader. Supernatant from 2% rat RBCs mixed with 0.1% Triton X-100 was used as a 100% hemolysis control and a supernatant from 2% rat RBCs in PBS buffer was used as a negative control.

12. Binding of Cyt2Aa2 toxin on rat RBC membrane

The 5 µg/ml of activated toxin was mixed with 2% rat RBC in PBS pH 7.4 in total volume 0.4 ml and incubated for 2 hours at room temperature in micro-centrifuge tube. The mixture was centrifuged at 12,000g for 30 minutes to separate pellet as the membrane-bound complexes from unbound toxin in supernatant before subjected to SDS-PAGE without heating. Proteins separated on SDS-PAGE were visualized by Coomassie blue stain and detected by western blotting using anti-Cyt2Aa2.

Copyright by Kasetsart University All rights reserved

13. Western blotting or immunoblotting

The nitrocellulose membrane, two fiber pads, and two Whatman papers (pre-cut) were placed in a shallow tray filled with Transfer Buffer for a few minutes. The stacking gel was cut off from SDS-PAGE gel with a clean razor blade and soak gel in Transfer Buffer for a few minutes. The transfer apparatus gel cassettes was opened with the black panel lying flat on the bottom of the tray filled with Transfer Buffer, the clear panel should be against the side of the tray. The transfer sandwich was prepared on the black panel in the tray filled with Transfer Buffer. one fiber pad, one Whatman papers, SDS gel, nitrocellulose membrane, one Whatman papers, one fiber pad. The air bubbles was removed by rolling a glass tube on the membrane. The sandwich was covered with the clear panel, fasten with the latch, and insert the gel cassette into the electrode module with the black panel facing the black cathode electrode panel. The bio-ice cooling unit was inserted into the buffer chamber, and filled the buffer chamber with Transfer Buffer, transferred for 70 minutes at 4 ºC, stirring at a constant current of 100V and then the membrane was washed with distilled water on the shaker for 10 minutes. The membrane was incubated with Blocking Buffer on a shaker at 37 °C for 30 minutes. The anti-Cyt2Aa2 was used as primary antibody, diluted to Blocking Buffer (1:5000) and incubated the membrane with the Blocking Buffer the diluted primary antibody on a shaker for overnight at 4 ºC. The membrane was washed two times with Blocking Buffer on the shaker for 10 minutes each time. Secondary antibody was diluted to Blocking Buffer (1:5000) and incubated the membrane with the diluted secondary antibody on a shaker at 37 °C for 1.30 hours. The membrane was washed two times with distilled water on the shaker for 5 minutes each time. The membrane was washed with 0.05% PBS-tween on the shaker for 5 minutes and incubated in AEC Substrate Reagent (4 ml deionized water, 2 drops Acetate Buffer, 1 drop AEC Chromogen, 1 drop hydrogen peroxide) at 37 °C for 15 minutes until clear red insoluble signal was obtained for positive control. The membrane was washed with steriled distilled water.

Copyright by Kasetsart University All rights reserved

RESULTS

1. Plasmid extraction

E. coli harboring *cyt2Aa2* wild type cell was grown to extract the plasmid pGEM-Cyt2Aa2 carrying the full-length *cyt2Aa2* gene. The plasmid was detected by gel electrophoresis of 0.8% agarose gels and compared to 1 kb of DNA marker. The plasmids pGEM-Cyt2Aa2 size was higher than 3.8 kb due to the plasmids without digestion (Figure 12).

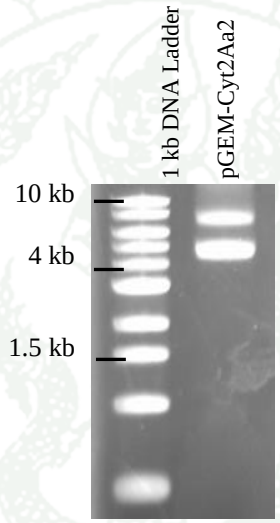

Figure 12 Recombinant plasmid pGEM-Cyt2Aa2 carrying the full-length *cyt2Aa2* gene without digestion.

2. Mutant construction

Site-directed mutagenesis was used to construct the Cyt2Aa2 mutants. The recombinant plasmid pGEM-cyt2Aa2 was used as a template for single substitutions I139A, S159A, L160A, S161A, A162V, D209N and V215A with appropriate primers described in Table 1. All of plasmids were successfully amplified by PCR with designed primers and yielded the products of the expected size at 3.8 kb (Figure 13) except S161A plasmid showed low yield. The PCR products showed more than one size due to the PCR products without digestion (Figure 13). The PCR products were

Copyright by Kasetsart University All rights reserved

digested with *DpnI* and transformed into competent *E.coli* cells. Three colonies of each mutants were subjected to plasmid extraction. DNA sequencing were performed to confirm mutant DNA sequence. All mutants were successfully constructed and verified by DNA sequencing (Appendix Figure 1 and 2).

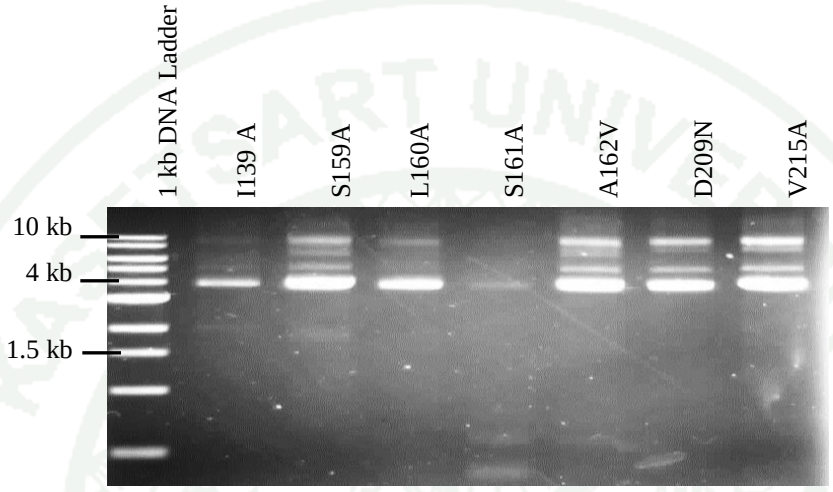

Figure 13 PCR products of CytAa2 mutants without DpnI digestion by agarose gel electrophoresis. All of plasmids were successfully amplified by PCR with designed primers and yielded the products of the expected size at 3.8 kb except S161A plasmid showed low yield.

3. Protein expression

3.1 Small scale protein expression

Three colonies of each mutant were verified by DNA sequencing. The correct DNA sequence of colony mutants are I139A (I139A-3), S159A (S159A-1, S159A-2, S159A-3), L160A (L160A-1, L160A-3), S161A (S161A-1, S161A-2), A162V (A162V-1, A162V-2, A162V-3), D209N (D209N-2, D209N-3) and V215A (V215A-1, V215A-2). The colonies of WT and mutants were picked and grown in 50 ml LB containing 100 µg/ml ampicillin and 0.1 mM IPTG to induce protein expression of each mutant colony. Total proteins were separated on 12% SDS-PAGE and visualized by Coomassie blue-R stain. Figure 14 shows that S159A-1 L160A-1

Copyright by Kasetsart University All rights reserved

S161A-1 A162V-1 D209N-2 and V215A-1 mutant colonies have comparable expression level with wild type. Large scale protein expression were performed. The I139A colony showed very low expression level, therefore this mutant was not included in next step.

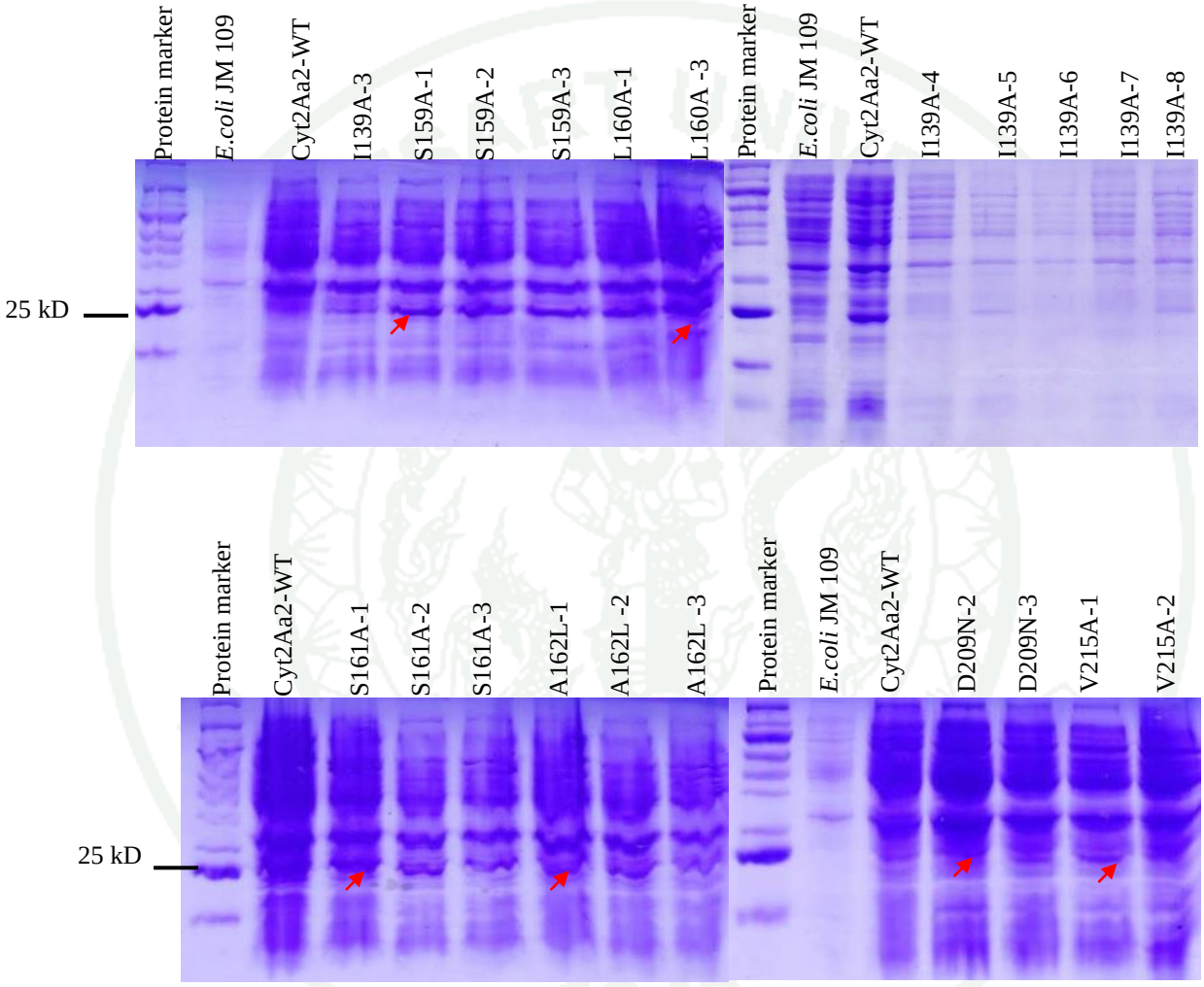

Figure 14 Small scale protein expression of Cyt2Aa2 wild type, mutants and *E.coli* JM 109 lysed cell. Arrows showed high expression of mutant colony.

Copyright by Kasetsart University All rights reserved

3.2 Large scale protein expression

The expression of all Cyt2Aa2 wild type and mutant proteins were induced by 1 mM IPTG and the cultures were grown at 37°C. The lysed cell, soluble fractions and inclusion bodies of all mutant and wild type were analyzed on 12% SDS-PAGE (Figure 15). Inclusion bodies of all mutant and wild type were detected by western blotting using anti-Cyt2Aa2 (Figure 16). All mutant proteins were expressed as inclusion bodies in *E. coli* similar to that of the wild type except I139A mutant that showed low protein expression level.

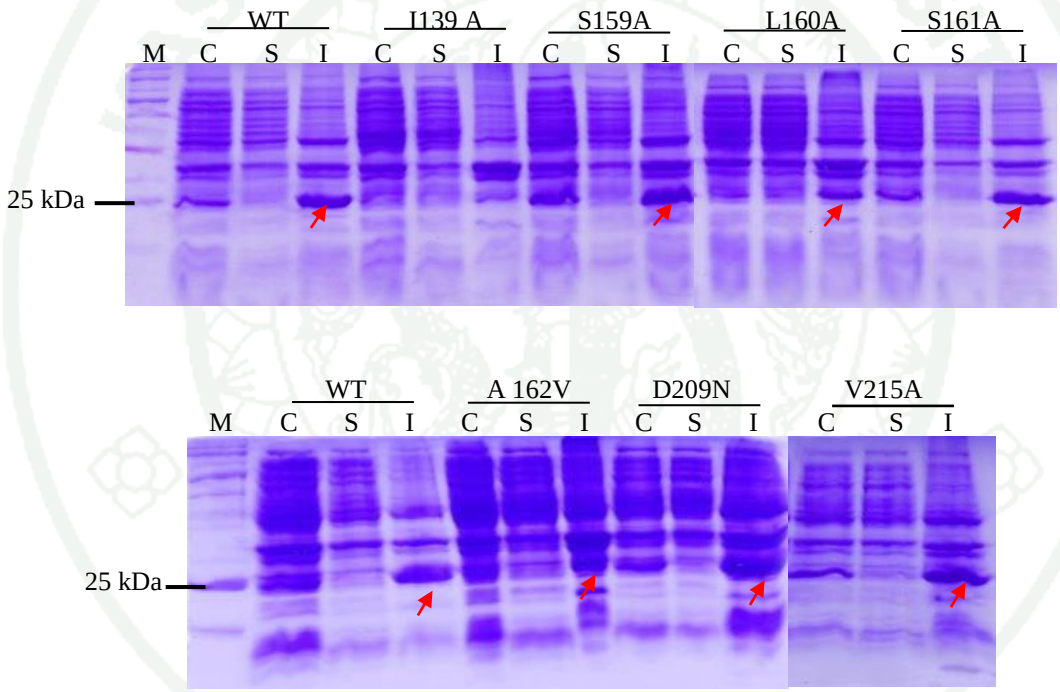

Figure 15 Protein expression of wild type (WT), I139A, S159A, L160A, S161A, A162V, D209N and V215A proteins. Lane M: Protein marker. After sonication, the lysed cell (C) was centrifuged to separate soluble fractions (S) and inclusion bodies (I). Arrows showed protein expression of mutant as inclusion bodies in *E. coli* similar to that of the wild type.

Copyright by Kasetsart University All rights reserved

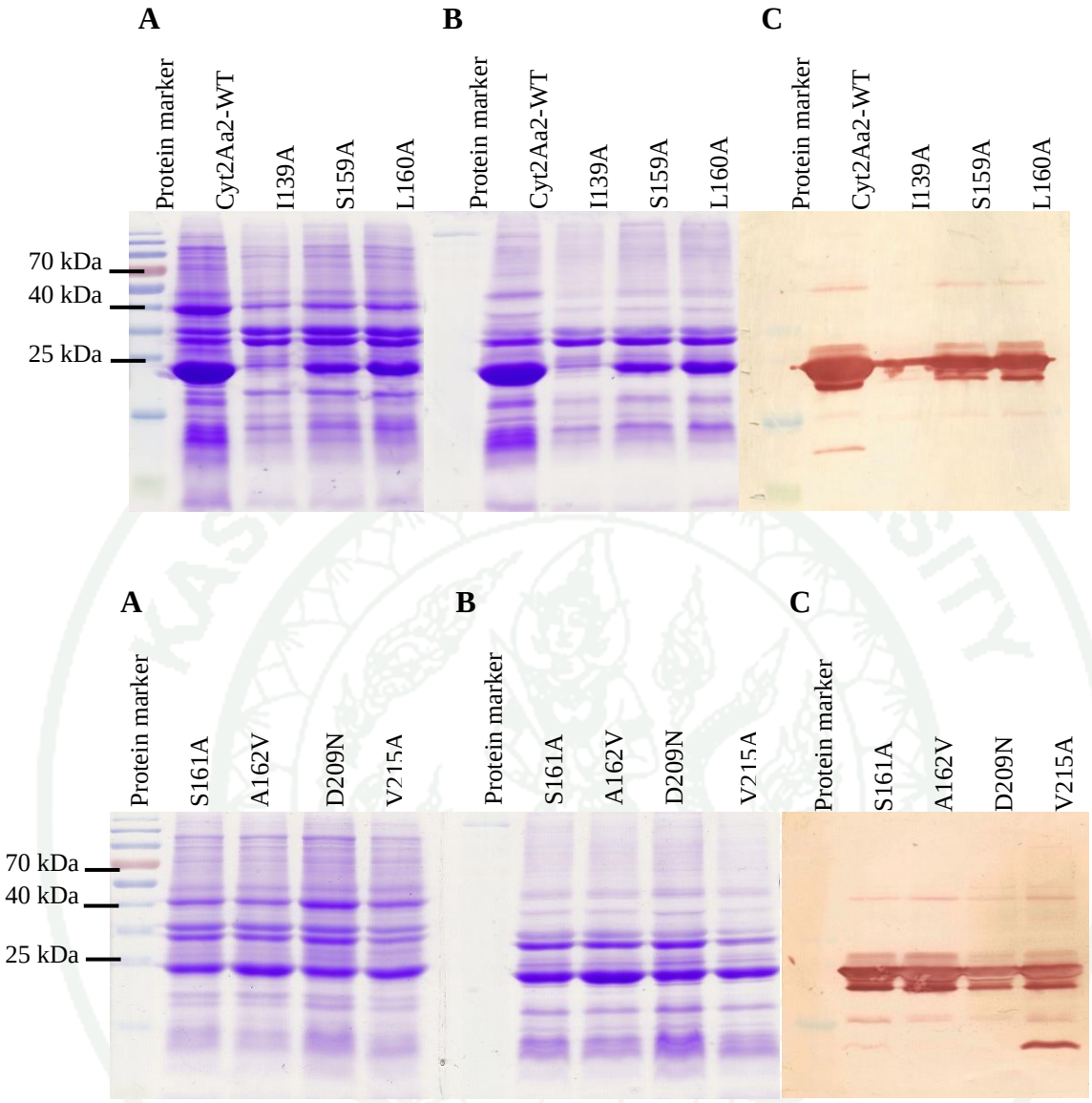

Figure 16 Inclusion bodies of wild type (WT) and mutants were visualized by western blotting detection using anti-Cyt2Aa2. A) SDS gel before western blotting, B) SDS gel after western blotting and C) membrane blotting.

4. Solubilization and activation of Cyt2Aa2

The inclusion body was solubilized in 50 mM carbonate buffer pH 10.5 at the ratio 1:1 inclusion to the buffer, incubated at 37 ^{o}C for 1 hour. All of mutant inclusions could solubilize as protoxin similar to the wild type except I139A and V215A. The protoxin of Cyt2Aa2 wild type and mutants were digested by proteinase K at the ratio

Copyright by Kasetsart University All rights reserved

100:1 (w/w) toxin to proteinase K for 1 hour at 37 ^{o}C. The activity of proteinase K was inhibited by 4 mM PMSF. All mutant was activated similar to that of wild type except I139A and V215A, that no protoxin were available. The solubility of protoxins and the activated toxins were analyzed on 12% SDS-PAGE (Figure 17) and detected by western blotting using anti-Cyt2Aa2 (Figure 18).

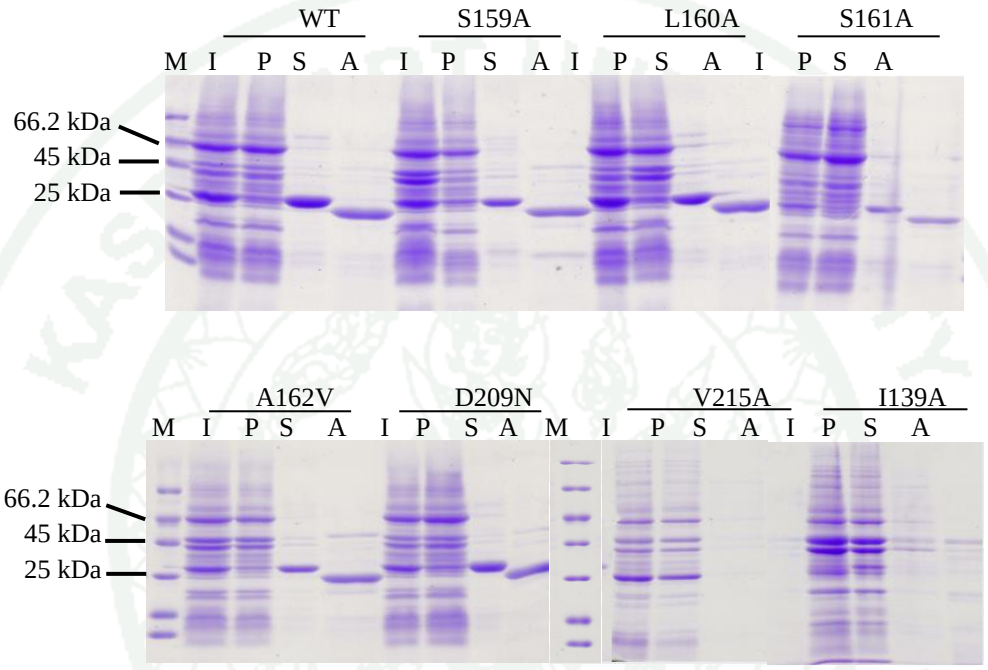

Figure 17 Solubilization and activation test of Cyt2Aa2 wild type (WT) and mutant toxins. Lane M: Protein marker. Inclusion bodies (I), the pellet (P) after solubilization in 50mM carbonate buffer at 37 ^{o}C for 1 hour. The soluble fractions (S) after solubilization in 50mM carbonate buffer. Activated toxins (A) were obtained from incubation of the soluble fraction with proteinase K at 37^{o}C for 1 hour.

Copyright by Kasetsart University All rights reserved

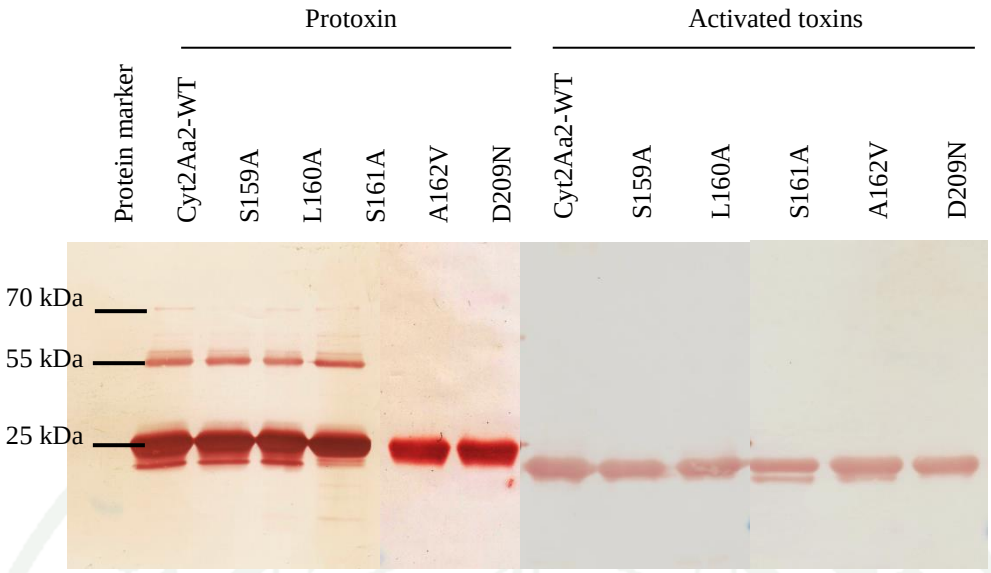

Figure 18 Cyt2Aa2 toxin detection by western blotting using anti-Cyt2Aa2 of protoxin and activated toxins of wild type (WT) and mutants.

5. Binding of Cyt2Aa2 toxin on rat RBC membrane

Five µg/ml of activated toxin was mixed with 2% rat RBC in PBS pH 7.4 in total volume 0.4 ml and incubated for 2 hours at room temperature. The membrane-bound complexes as pellet was separated from unbound toxin in supernatant. The membrane-bound complexes was subjected to 12% SDS-PAGE without heating and detected by western blotting using anti-Cyt2Aa2. Large complexes of Cyt2Aa2 wild type on RBC membrane were clearly observed from western blotting detection using anti-Cyt2Aa2. The S159A, L160A and S161A formed fewer complexes on RBCs than that of the wild type. In contrast, the inactive mutant A162V and D209N were unable to lyse red blood cells and complexes were not detected (Figure 19).

Copyright by Kasetsart University All rights reserved

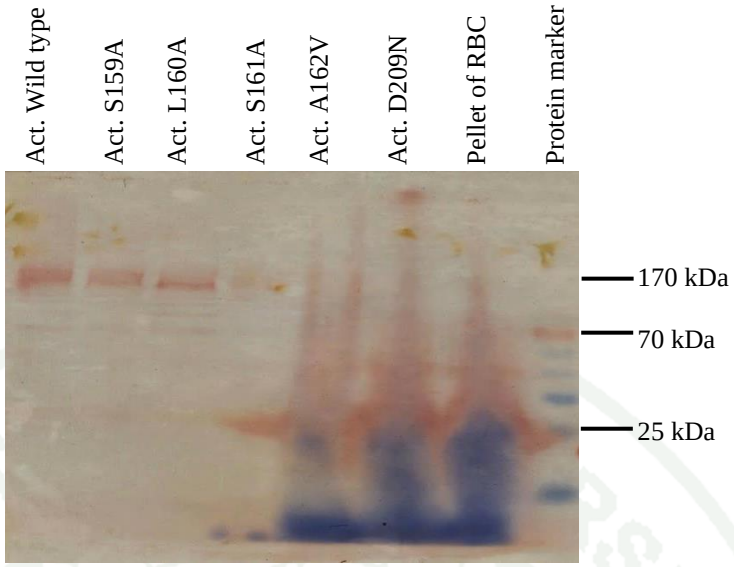

Figure 19 Membrane binding and complex formation of Cyt2Aa2 wild type and mutant toxins on rat RBC membrane. Activated toxin was mixed with 2% rat RBC in PBS pH 7.4 in total volume 0.4 ml and incubated for 2 hours at room temperature. The membrane-bound toxin complexes were visualized by western blotting using anti-Cyt2Aa2. Rat RBCs incubated without toxin was used as a negative control.

6. Larvicidal and hemolytic activity of mutant proteins

The 3rd instar *A. aegypti* larvae were fed with two-fold serial dilutions of toxin inclusions from 0.12 to 250 µg/ml diluted in distilled water. One ml of the serial diluted inclusion was added to a 24-well plate containing 10 larvae in 1 ml of distilled water. The mortality was recorded after 24 hours of incubation at room temperature and LC_{50} value was determined by Probit analysis. Mosquito-larvicidal activity of S159A, L160A S161A and D209N mutants are lower than that of wild type. The I139A A162V and V215A mutants showed no toxicity even increased the concentration of those mutants up to 250 µg/ml (Table 2).

Copyright by Kasetsart University All rights reserved

Table 2 Mosquito-larvicidal and hemolytic activities of Cyt2Aa2 wild type and mutants against *A. aegypti* larvae and RBC.

Toxin	Protein Expression	Solubility	Activation	Hemolytic end-point (µg/ml)	Larvicidal activity LC_{50} (µg/ml)
WT	Yes	+++	Yes	0.05-0.1	0.6 (0.5-0.7)
I139A	Low	_	nd	nd	Non toxic
S159A	Yes	+++	Yes	0.1-0.2	1.3(1.0-1.6)
L160A	Yes	+++	Yes	0.1-0.2	1.3 (1.0-1.6)
S161A	Yes	+++	Yes	0.2-0.4	1.7 (1.2-2.2)
A162V	Yes	+++	Yes	No lysis	Non toxic
D209N	Yes	+++	Yes	No lysis	1.3 (0.9-1.7)
V215A	Yes	_	nd	nd	Non toxic

*nd, not determined because there was no activated toxin for the assay.

The inclusion bodies was solubilized in 50 mM bicarbonate buffer pH 10.5 at 37 ^{o}C for 1 hour. The protoxin of Cyt2Aa2 and mutants were digested by proteinase K at 37 ^{o}C for 1 hour. Hemolytic assays were performed by adding the two-fold serial dilutions of the activated Cyt2Aa2 wild type or its mutants from 0.024 to 50 µg/ml diluted in PBS pH 7.4 in a 96-well microtiter plate. One hundred µl of the serial diluted toxin was mixed with 100 µl of 2% RBC. The hemolytic endpoint was monitored after incubation for 24 hours at room temperature. Hemolytic activity of the activated Cyt2Aa2 toxin against rat RBC was tested in a microtiter plate. Lower hemolytic activity was observed for the S159A, L160A and S161A mutants and no hemolysis was detected for the A162V and D209N mutants (Table 2). This result was consistent to the hemoglobin release assay in which the A162V and D209N mutant could not completely break rat RBC even when used at high toxin concentration up to 12 µg/ml (Figure 20) and these mutants were unable to lyse red blood cells.

Copyright by Kasetsart University. All rights reserved

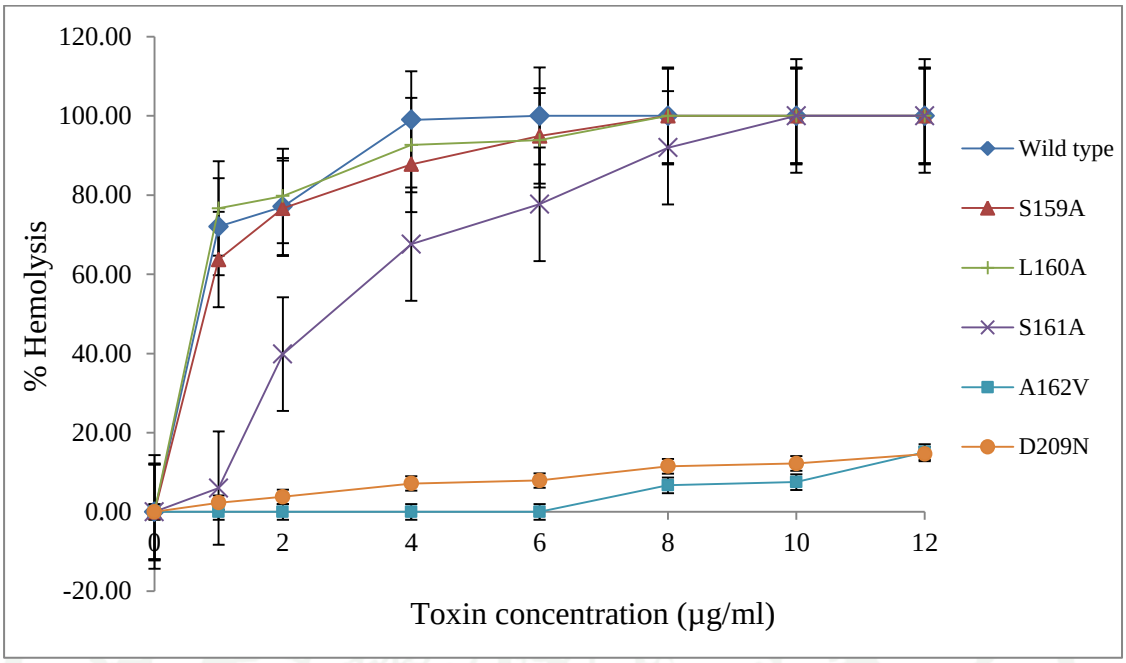

Figure 20 Hemoglobin release assay of rat RBCs treated with Cyt2Aa2 wild type and Cyt2Aa2 mutant toxins at room temperature for 2 hours. The percentage of hemolysis was calculated from the absorption of hemoglobin at 540 nm. Supernatant from 2% rat RBCs mixed with 0.1% Triton X-100 used as a 100% hemolysis control and a supernatant from 2% rat RBCs in PBS buffer was used as a blank

Copyright by Kasetsart University All rights reserved

DISCUSSION

Cyt2Aa2 is specifically toxic against dipteran larvae *in vivo,* and also active to several cell types such as erythrocytes (Promdonkoy *et al.*, 2003). Cyt2Aa2 show identical to Cyt2Aa1 from *B. thuringiensis* subsp. *kyushuensis,* both toxins should adopt a similar α/β structure containing 6 α-helices and 7 β-sheets (Koni *et al.*, 1993; Promdonkoy *et al.*, 2004). It has been proposed that β5, β6 and β7 are long enough to span the membrane should insert into the membrane (Promdonkoy and Ellar, 2000). The possible roles of amino acids in αA-αD may involve with binding onto the cell membrane, the oligomerization of toxin molecules to generate pore and αD-β4 loop and β6-β7 loop could facilitate conformational changes during membrane insertion of β-sheets (Promdonkoy *et al.,* 2005; 2000). Cyt toxin is structurally related to a few toxins, volvatoxin A2 (VVA) (Lin *et al.,* 2004) and Evf toxin. Mapping between Cyt and Evf toxins revealed that the lipid binding cavity of Cyt toxin might locate on αD (I139), loop between αD and β4, and β7 (V215). Also, the electrostatic surface was identified in Cyt and was proposed that these residues, V150, N159, L160 and D209 were involved with lipid binding pocket (Rigden *et al.,* 2009). This study attempts to elucidate the role of expected membrane binding residues whether these residues are important for binding and activity of Cyt toxin. To investigate this possibility, selected amino acids were substituted (I139A in alpha-D, S159A, L160A, S161A and A162V on loop between β4 and β5, and D209N and V215A on β7).

The expression of all Cyt2Aa2 wild type and mutant proteins were induced by 1 mM IPTG and the cultures were grown at 37°C. Analysis of the whole cell lysate on SDS-PAGE (Figure 15) revealed that all mutants expressed at high level similar to that of wild type toxin except I139A mutant showed low level of protein expression. Substitution I139 by alanine in alpha-D may affect protein folding and inclusion formation. These residues are located in the hydrophobic face of helix alpha-D pointing inside the molecule. Replacement this positions with smaller and less hydrophobic side-chain may destabilize the van der Waal contact which is required to hold the right conformation. The 6 mutants (S159A, L160A, S161A, A162V D209N and V215A) were produced as inclusion bodies similar to that of wild type. Solubility

Copyright by Kasetsart University. All rights reserved

test in 50 mM carbonate buffer (Na_2CO_3/$NaHCO_3$) pH 10.5 revealed that 5 mutants (S159A, L160A, S161A, A162V and D209N) could solubilize in the carbonate buffer similar but V215A mutant were unable to solubilize. Substitution V215 by alanine on beta-7 may affect protein folding and inclusion formation. Replacement this positions with smaller and less hydrophobic side-chain may destabilize the van der Waal contact which is required to hold the right conformation lead to misfolding and alteration of the three dimensional structure.The misfold protein may not be solubilized in normal buffer. This result demonstrated that V215 is critical residues playing important role to maintain structural folding of the toxin. The soluble proteins from 5 mutants were activated by proteinase K (1%, w/w) at 37 ^{o}C for 1 hour. All of them were processed and yielded similar product to that of wild type. Results indicated that the replacement at these positions (S159A, L160A, S161A, A162V and D209N) maybe not affect the folding of the toxin that the conformation of these mutants might not different from that of wild type..

Mosquito-larvicidal activity of insecticidal crystal proteins is normally tested by feeding the larvae with the toxin inclusions (Schnepf *et al*., 1998). It was found that Cyt2Aa2 inclusion is highly toxic to *A. aegypti* larvae (Promdonkoy *et al*., 2003). The protease activated form of mutant toxins exhibited comparable hemolytic activity to wild type. Replacement at I139A and V215A positions of Cyt2Aa2 yielded the toxin inclusions that are less soluble or insoluble in carbonate buffer. Hemolytic activity of these mutants could not be accessed because no activated toxin was available. These mutants also exhibited no larvicidal activity (Table 2).

Mutant inclusions that were solubilized in carbonate buffer showed different toxicity of hemolytic and larvicidal activity (Table 2). Mutant S159A, L160A and S161A showed high hemolytic activity consistent with hemoglobin release assay that could completely break RBC. However these mutants showed low toxicity against *A. aegypti*. Binding assay with rat RBC of these mutants showed lower binding and oligomerization to that of wild type. These results suggest that replacement of S159, L160 and S161 by alanine on loop between beta-4 and beta-5 could reduce reduce the binding to RBC membrane, oligomerization and activity of the toxin. A substitution of these positions may interrupt their hydrogen bonding between the loop and the core

Copyright by Kasetsart University All rights reserved

beta sheet, leading to molecular destabilizing of the toxin. This destabilization also affected an ability to bind and form complexes on red blood cells.

Hemoglobin release assay demonstrated that A162V and D209N could not break RBC even at high concentration. These mutants were unable to lyse red blood cells and showed no hemolytic activity. This result was considered that there are two possibility way, these mutants could interfere membrane binding and oligomerization of the toxin, or these mutants could bind on cell membrane but not form complexes as oligomer of the toxin on rat red blood cells. The mutant A162V showed no toxicity against *A. aegypti*, but D209N showed low toxicity against *A. aegypti*. It is possible that this mutant's different toxicity affinities to cells from various sources might be caused by differences in membrane composition as previously described (Chow *et al.*, 1989). Major components found in cell membrane are phosphatidylcholine (PC), phosphatidylethanolamine (PE), sphingomyelin and cholesterols, cell membranes contain many other lipids, albeit in lower amounts (Valcarcel *et al.*, 2001). Analysis of phospholipid compositions in *A. aegypti* cells found PE and PC as major components in membrane fractions (Butters and Hughes, 1981; Jones *et al*., 1992), whereas PE and sphingomyelin are major phospholipids found in rat red blood cell membranes (Virtanen *et al*., 1998). A study of lipid polymorphism of erythrocytes found that the erythrocyte membrane contains many different species of lipids more than 100 types. The different lipid compositions could provide appropriate fluidity characteristics as well as presenting the varying lipid physical properties (Cullis and Kruijff, 1979; Cullis *et al.*, 1986). Replacement A162 by valine on loop between beta-4 and beta-5 could not retain membrane binding, oligomerization and activity of the toxin.
A substitution of this alanine with bigger and more hydrophobic side-chain may interrupt their hydrogen bonding between the loop and the beta sheet, also affected an ability to bind and form complexes on red blood cells. In contrast, the replacement D209 by asparagine on beta-7 could retain larvicidal activity of the toxin. The polarity of asparagine also affected to larvicidal activity of the toxin. However, binding and oligomerization to red blood cell and mosquito larval cell membranes may not be the same because of the differences of membrane compositions. It could be possible that other membrane components such as glycoproteins and lipoproteins contribute in some ways to the binding of the toxin (Suktham *et al.*, 2013).

Copyright by Kasetsart University All rights reserved

CONCLUSION

All mutants (I139A, S159A, L160A, S161A, A162V, D209N and V215A) were successfully constructed, these mutants could express at high level similar to the wild type toxin except I139A mutant showed low protein expression level. All mutants were produced as inclusion bodies similar to that of wild type. The 5 mutants (S159A, L160A, S161A, A162V and D209N) could be solubilized in 50 mM carbonate buffer similar to the wild type, whereas V215A was unable to solubilize. The soluble proteins from 5 mutants were activated by proteinase K. All of them were processed and yielded similar product to that of the wild type.

Hemolytic activity of mutant I139A and V215A could not be accessed because no activated toxin was available, these mutants exhibited no larvicidal activity. Mutant S159A, L160A and S161A showed high hemolytic activity but low toxicity against *A. aegypti*, and binding assay of these mutants with rat RBC showed lower binding and oligomerization to that of the wild type. Hemoglobin release assay demonstrated that A162V and D209N could not completely break RBC even when use at high concentration and that showed no hemolytic activity, and these mutants could interfere membrane binding and oligomerization of the toxin. The mutant A162V showed non toxicity against *A. aegypti*, but D209N could low toxic against *A. aegypti*.

Results presented here clearly demonstrated that amino acids in αD, loop between β4 and β5, and β7 of Cyt2Aa2 toxin are important in membrane binding as well as complex formation. Substitution of amino acids in this region alters the biological activity. Selectivity of the toxin to certain target cells might be improved by amino acid replacement in this region.

Copyright by Kasetsart University All rights reserved

LITERATURE CITED

Altschul, S.F., T.L. Madden, A.A. Schaffer, J. Zhang, Z. Zhang, W. Miller and D.J. Lipman. 1997. Gapped BLAST and PSI-BLAST: a new generation of protein database search programs. **Nucleic Acids Res.** 25; 3389–3402.

Ash, C., J.A.E. Farrow, S.Wallbanks and M.D. Collins. 1991. Phylogenetic hetero geneity of the *genus Bacillus* revealed by comparative analysis of small subunit ribosomal RNA sequences. **Lett Appl Microbiol**. 13: 202–206.

Basset, A., P. Tzou, B. Lemaitre and F. Boccard. 2003. A single gene that promotes interaction of a phytopathogenic bacterium with its insect vector, *Drosophila melanogaster*. **EMBO Rep.** 4: 205–209.

Berbert-Molina, M.A., A.M.R. Prata, L.G. Pessanha and M.M. Silveira. 2008. Kinetics of *Bacillus thuringiensis var. israelensis* growth on high glucose concentrations. **J Ind Microbiol Biotechnol** 35 (11): 1397–1404.

Berman, H., K. Henrick, H. Nakamura and J.L. Markley. 2007. The worldwide Protein Data Bank (wwPDB): ensuring a single, uniform archive of PDB data.**Nucleic Acids Res.** 35: D301–D303.

Bravo, A., S. Likitvivatanavong, S.S. Gill and M. Soberón. 2011. *Bacillus thuringiensis*: a story of a successful bioinsecticide**. Insect. Biochem. Mol. Biol**. 41: 423–431.

Bulla, L.A., D.B. Bechtel, K.J. Kramer, Y.I. Shethna, A.I. Aronson and A.I. Fitz-James. 1980. Ultrastructure, physiology and biochemistry of *Bacillus thuringiensis*. **Crit Rev Microbiol.** 8: 147–204.

Butko, P. 2003. Cytolytic toxin Cyt1A and its mechanism of membrane damage: data and hypotheses. **Appl. Environ. Microbiol**. 69: 2415–2422.

Copyright by Kasetsart University All rights reserved

Butters, T.D., and R.C. Hughes. 1981. Phospholipids and glycolipids in subcellular fractions of mosquito *Aedes aegypticells*. **In Vitro Cell. Dev. Biol.** 17: 831–838.

Chow, E., G.J. Singh, and S.S. Gill. 1989. Binding and aggregation of the 25-kilodalton toxin of *Bacillus thuringiensis* subsp. *israelensis* to cell membranes and alteration by monoclonal antibodies and amino acid modifiers. **Appl. Environ. Microbiol**. 55: 2779–2788.

Clamp, M., J. Cuff, S.M. Searle and G.J. Barton. 2004. The Jalview Java alignment editor. **Bioinformatics**. 20: 426–427.

Cohen, S., O. Dym, S. Albeck, E. Ben-Dov, R. Cahan, M. Firer and A. Zaritsky. 2008. High-resolution crystal structure of activated Cyt2Ba monomer from B. *thuringiensis* subsp. *israelensis*. **J. Mol. Biol.** 380: 820–827.

Cullis, P.R. and B. de Kruijff. 1979. Lipid polymorphism and the functional roles of lipids in biological membranes. **Biochim. Biophys. Acta**. 559: 399–420.

Cullis, P.R., M.J. Hope and C.P.Tilcock. 1986. Lipid polymorphism and the roles of lipids in membranes. **Chem. Phys. Lipids**. 40: 127–144.

DeLano, W.L. 2002. The PyMOL Molecular Graphics System on the World Wide. Source: http://www.pymol.org.

Drobniewski, F.A. and D.J. Ellar. 1989. Purification and properties of a 28-kilodalton hemolytic and mosquitocidal protein toxin of *Bacillus thuringiensis* subsp. *darmstadiensis* 73-E10-2. **J Bacteriol**. 171: 3060–3067.

Du, J., B.H. Knowles, J.Li and D.J. Ellar. 1999. Biochemical characterization of *Bacillus thuringiensis* cytolytic toxins in association with phospholipid bilayer. **Biochem. J**. 338: 185–193.

Copyright by Kasetsart University All rights reserved

Edgar, R.C. 2004. MUSCLE: multiple sequence alignment with high accuracy and high throughput. **Nucleic Acids Res.** 32: 1792–1797.

Garbeva, P., J.A. van Veen and J.D. van Elsas. 2003. Predominant Bacillus spp. in agricultural soil under different management regimes detected via PCR-DGGE. **Microb Ecol.**45: 302–316.

Giacomodonato, M.N., M.J. Pettinari, I.S. Guadalupe, S.M. Beatriz and N.I. Lopez. 2001. A PCR- based method for the screening of bacterial strains with antifungal activity in suppressive soybean rhizosphere. **World J Microbiol Biotechno**.17: 51–55.

Guerchicoff, A., A. Delecluse and C.P. Rubinstein. 2001. The *Bacillus thuringiensis* cyt genes for hemolytic endotoxins constitute a gene family. **Appl. Environ. Microbiol.** 67: 1090–1096.

Hamilton, J.A. 2004. Fatty acid interactions with proteins: what X-ray crystal and NMR solution structures tell us. **Prog. Lipid Res**. 43: 177–199.

Holm, L. and C. Sander. 1993. Protein structure comparison by alignment of distance matrices. **J. Mol. Biol.** 233: 123–138.

Jones, H.E., J.L. Harwood, I.D. Bowen and G. Griffiths. 1992. Lipid composition of subcellular membranes from larvae and prepupae of *Drosophila melanogaster*. **Lipids.** 27: 984–987.

Knowles, B.H. and D.J. Ellar. 1987. Colloid-osmotic lysis is a general feature of the mechanism of action of *Bacillus thuringiensis* δ-endotoxin with different specificity. **Biochem. Biophys. Acta** 924: 509-518.

Copyright by Kasetsart University All rights reserved

Koni, P.A. and D.J. Ellar. 1993. Cloning and characterization of a novel *Bacillus thuringiensis* cytolytic δ-endotoxins. **J. Mol. Biol**. 229: 319-327.
Krissinel, E. and K. Henrick. 2004. Secondary-structure matching (SSM), a new tool for fast protein structure alignment in three dimensions. **Biol. Crystallogr.** 60: 2256–2268.

Landau, M., I. Mayrose, Y. Rosenberg, F. Glaser, E. Martz, T. Pupko and N. BenTal. 2005. ConSurf 2005: the projection of evolutionary conservation scores of residues on protein structures. **Nucleic Acids Res**. 33: W299–W302.

Lecadet, M.M., E. Frachon, V.C. Dumanoir, H. Ripouteau, S. Hamon, P. Laurent and I. Thiery. 1999. Updating the H-antigen classification of *Bacillus thuringiensis*. **J Appl Microbiol**. 86: 660–672.

Li, J., D.J. Derbyshire, B. Promdonkoy and D.J. Ellar. 2001. Structural implication for the transformation of the *Bacillus thurengiensis* δ-endotoxins from water-soluble to membran-inserted forms. **Biochemical society**. 29: 571-577.

Li, J., P.A. Koni and D.J. Ellar. 1996. Structure of the Mosquitocidal d-endotoxin from *Bacillus thuringiensis* sp. *kyushuensis* and implications for membrane pore formation. **J. Mol. Biol**. 257: 129–152.

Lin, S.C., Y.C. Lo, J.Y. Lin and Y.C. Liaw. 2004. Crystal structures and electron micrographs of fungal valvotoxin A. **J. Mol. Biol.** 343: 477–491.

Manceva, S.D., D. J. Pusztai-Carey, P.S. Russo and P. Butko. 2005. A detergent-like mechanism of action of the cytolytic toxin Cyt1A from *B. thuringiensis* var. *israelensis*. **Biochemistry** 44: 589–597.

Milner, R.J. 1994. History of *Bacillus thuringiensis*. **Agric Ecosyst Environ**. 49(1): 9–13.

Copyright by Kasetsart University All rights reserved

Murzin, A.G. 1993. Sweet-tasting protein monellin is related to the cystatin family of thiol proteinase inhibitors. **J. Mol. Biol**. 230: 689–694.

Novotny, M., D. Madsen and G.J. Kleywegt. 2004. Evaluation of protein fold comparison servers. **Proteins.** 54: 260–270.

Parker, M.W. and S.C. Feil. 2005. Pore-forming protein toxins: from structure to function. **Progr. Biophys. Mol. Biol**. 88: 91–142.

Perez, C., C. Munoz-Garay, L.C. Portugal, J. Sanchez, S.S. Gill, M. Soberon and A. Bravo. 2007. *Bacillus thuringiensis* ssp. *israelensis* Cyt1Aa enhances activity of Cry11Aa toxin by facilitating the formation of a pre-pore oligomeric structure. **Cell Microbiol.** 9: 2931–2937.

Perez, C., L.E. Fernandez, J. Sun, J.L. Folch, S.S. Gill, M. Soberon and A. Bravo. 2005. *Bacillus thuringiensis* subsp. israelensis Cyt1Aa synergizes Cry11Aa toxin by functioning as a membrane-bound receptor. **Proc. Natl. Acad. Sci. USA**. 102: 18303–18308.

Promdonkoy, B. and D.J. Ellar. 2000. Membrane pore architecture of a cytolytic toxin from *Bacillus thuringiensis*. **Biochem J**. 350(1): 82–275.

Promdonkoy, B. and D.J. Ellar. 2005. Structure-function relationships of a membrane pore forming toxin by reversion mutagenesis. **Molecular Membrane Biology**. 22(4): 327-337.

Promdonkoy, B., N. Chewawiwat, S.Tanapongpipat, P. Luxananil and S. Panyim. 2003. Cloning and characterization of a cytolytic and mosquito larvicidal δ-endotoxin from *Bacillus thuringiensis* subsp. *darmstadiensis*. **Current Microbiology.** 46: 94–98.

Copyright by Kasetsart University All rights reserved

Promdonkoy, B., W. Pathaichindachote, C. Krittanai, M. Audtho, N. Chewawiwat and S. Panyim. 2004. Trp132, Trp154, and Trp157 are essential for folding and activity of a Cyt toxin from *Bacillus thuringiensis*. **Biochemical and Biophysical Research Communications** 317: 744–748.

Quevillon-Cheruel, S., N. Leulliot, C.A. Muniz, M. Vincent, J. Gallay, M. Argentini, D. Cornu, F. Boccard, B. Lemaître and H. van Tilbeurgh. 2009. Evf, a virulence factor produced by the Drosophila pathogen *Erwinia carotovora*, is an S palmitoylated protein with a new fold that binds to lipid vesicles. **J. Biol. Chem.** 284(6): 3552-3562.

Ragni, A., I. Thiery and A. Delecluse. 1996. Characterization of six highly mosquitocidal Bacillus thuringiensis strains that do not belong to the H-14 serotype. **Cur. Microbiol** 32: 48–54.

Rodriguez-Almazán, C., I. Ruiz de Escudero, E. C. Canton, Muñóz-Garay, C.Pérez, S.S. Gill, M. Soberón and M. Bravo. 2011. The amino- and carboxyl-terminal fragments of the *Bacillus thuringiensis* Cyt1Aa toxin have differential roles on toxin oligomerization and pore formation. **Biochemistry**. 50: 388-396.

Schnepf, H.E., N. Crickmore, J. Van Rie, D. Lereclus, J. Baum, J. Feitelson, D. Zeigler, and D.H. Dean. 1998. *Bacillus thuringiensis* and its pesticidal proteins. **Microbiol Mol Biol Rev** 62: 775–806.

Soufiane, B. and J.C. Cote. 2009. Discrimination among *Bacillus thuringiensis* H serotypes, serovars and strains based on 16S rRNA, *gyrB* and *aroE* gene sequence analyses. **Antonie Van Leeuwenhoek**. 95: 33–45.

Suktham, K., W. Pathaichindachote, B. Promdonkoy and C. Krittanai. 2013. Essential role of amino acids in αD–β4 loop of a *Bacillus thuringiensis* Cyt2Aa toxin in binding and complex formation on lipid membrane. **Toxicon.** 4663: 1–8.

Copyright by Kasetsart University All rights reserved

Thomas, W.E. and D.J. Ellar. 1983. Mechanism of action of *Bacillus thuringiensis var israelensis* insecticidal delta-endotoxin. **FEBS Lett.** 154: 362–368.

Valcarcel, C.A., M. Dalla Serra, C. Potrich, I. Bernhart, M. Tejuca, D. Martinez, F. Pazos, M.E. Lanio and G. Menestrina. 2001. Effects of lipid composition on membrane permeabilization by sticholysin I and II, two cytolysins of the sea anemone Stichodactyla helianthus. **Biophys. J**. 80: 2761–2774.

Virtanen, J. A., K.H. Cheng and P. Somerharju. 1998. Phospholipid composition of the mammalian red cell membrane can be rationalized by a superlattice model. **Proc. Natl. Acad. Sci.** 95: 4964–4969.

Ward, E.S., D.J. Ellar and C.N. Chilcott. 1988. Single amino acid changes in the *Bacillus thuringiensis var. israelensis* delta-endotoxin affect the toxicity and expression of the protein. **J. Mol. Biol**. 202: 527–535.

Weng, Y.P., Y.P. Lin, C.I. Hsu and J.Y. Lin. 2004. Functional domains of a pore-forming cardiotoxic protein, volvatoxin A2. **J. Biol. Chem**. 279: 6805–6814.

Wheeler, D.L., T. Barrett, D.A. Benson, S.H. Bryant, K. Canese, V. Chetvernin, D.M. Church, M. DiCuccio, R. Edgar, S. Federhen, L.Y. Geer, Y. Kapustin, O. Khovayko, D. Landsman, D.J. Lipman, T.L. Madden, D.R. Maglott, J. Ostell, V. Miller, K.D. Pruitt, G.D. Schuler, E. Sequeira, S.T. Sherry, K. Sirotkin, A. Souvorov, G. Starchenko, R.L. Tatusov, T.A. Tatusova, L. Wagner and E.Yaschenko. 2007. Database resources of the National Center for Biotechnology Information. **Nucleic Acids Res.** 35: D5–D12.

Ye, Y. and A. Godzik. 2003. Flexible structure alignment by chaining aligned fragment pairs allowing twists. **Bioinformatics.** 19(2): ii246–ii255.

Zheng, L., U. Baumann and U. Reymond. 2009. An efficient one-step site-directed and site-saturation mutagenesis protocol. **Nucl. Acids Res.** 32: 115.

Copyright by Kasetsart University All rights reserved

Zhu, J. and Z. Weng. 2005. FAST: a novel protein structure alignment algorithm. **Proteins.** 58: 618–627.

Copyright by Kasetsart University All rights reserved

APPENDICES

Copyright by Kasetsart University All rights reserved

Appendix A

Nucleotide sequences of Cyt2Aa2 wild type and mutants

Copyright by Kasetsart University All rights reserved

>Cyt2Aa2_WT

ATGTATACTAAAAATTTTAGTAATTCCAGAATGGAAGTAAAAGGTAATAACGGGTGTTCTG
CACCTATTATTAGAAAACCATTTAAACATATTGTATTAACGGTTCCATCCAGTGATTTAGAT
AATTTTAATACAGTCTTTTATGTACAACCACAATACATTAATCAGGCTCTTCATTTAGCAAA
TGCTTTTCAAGGGGCTATAGACCCACTTAATTTAAATTTCAATTTTGAAAAGGCACTCCAAA
TTGCAAATGGTATTCCTAATTCTGCAATTGTAAAAACTCTTAATCAAAGTGTTATACAGCAA
ACAGTTGAAATTTCAGTTATGGTTGAGCAACTTAAAAAGATTATTCAAGAGGTTTTAGGAC
TTGTTATTAACAGTACTAGTTTTTGGAATTCGGTAGAAGCTACAATTAAAGGCACATTTACA
AATTTAGACACTCAAATAGATGAAGCATGGATTTTTTGGCATAGTTTATCCGCCCACAATA
CAAGTTATTATTATAATATTTTATTTTCTATTCAAAATGAAGATACAGGTGCAGTTATGGCA
GTATTACCTTTAGCATTTGAGGTTTCTGTGGATGTTGAAAAACAAAAAGTATTATTCTTTAC
AATAAAAGATAGTGCACGATATGAAGTTAAAATGAAAGCTTTGACTTTAGTTCAAGCTCTA
CATTCCTCTAATGCCCCAATTGTAGATATATTTAATGTTAATAACTATAATTTATACCATTC
TAATCATAAGATTATTCAAAATTTAAATTTATCGAATTGA

Appendix Figure A1 Nucleotide sequences of Cyt2Aa2 wild type from DNA sequencing

> Cyt2Aa2_I139A

ATGTATACTAAAAATTTTAGTAATTCCAGAATGGAAGTAAAAGGTAATAACGGGTGTTCTG
CACCTATTATTAGAAAACCATTTAAACATATTGTATTAACGGTTCCATCCAGTGATTTAGAT
AATTTTAATACAGTCTTTTATGTACAACCACAATACATTAATCAGGCTCTTCATTTAGCAAA
TGCTTTTCAAGGGGCTATAGACCCACTTAATTTAAATTTCAATTTTGAAAAGGCACTCCAAA
TTGCAAATGGTATTCCTAATTCTGCAATTGTAAAAACTCTTAATCAAAGTGTTATACAGCAA
ACAGTTGAAATTTCAGTTATGGTTGAGCAACTTAAAAAGATTATTCAAGAGGTTTTAGGAC
TTGTTATTAACAGTACTAGTTTTTGGAATTCGGTAGAAGCTACAGCTAAAGGCACATTTAC
AAATTTAGACACTCAAATAGATGAAGCATGGATTTTTTGGCATAGTTTATCCGCCCACAAT
ACAAGTTATTATTATAATATTTTATTTTCTATTCAAAATGAAGATACAGGTGCAGTTATGGC
AGTATTACCTTTAGCATTTGAGGTTTCTGTGGATGTTGAAAAACAAAAAGTATTATTCTTTA
CAATAAAAGATAGTGCACGATATGAAGTTAAAATGAAAGCTTTGACTTTAGTTCAAGCTCT
ACATTCCTCTAATGCCCCAATTGTAGATATATTTAATGTTAATAACTATAATTTATACCATT
CTAATCATAAGATTATTCAAAATTTAAATTTATCGAATTGA

Appendix Figure A2 Nucleotide sequences of I139A mutant from DNA sequencing

Copyright by Kasetsart University All rights reserved

> Cyt2Aa2_S159A

ATGTATACTAAAAATTTTAGTAATTCCAGAATGGAAGTAAAAGGTAATAACGGGTGTTCTG
CACCTATTATTAGAAAACCATTTAAACATATTGTATTAACGGTTCCATCCAGTGATTTAGAT
AATTTTAATACAGTCTTTTATGTACAACCACAATACATTAATCAGGCTCTTCATTTAGCAAA
TGCTTTTCAAGGGGCTATAGACCCACTTAATTTAAATTTCAATTTTGAAAAGGCACTCCAAA
TTGCAAATGGTATTCCTAATTCTGCAATTGTAAAAACTCTTAATCAAAGTGTTATACAGCAA
ACAGTTGAAATTTCAGTTATGGTTGAGCAACTTAAAAAGATTATTCAAGAGGTTTTAGGAC
TTGTTATTAACAGTACTAGTTTTTGGAATTCGGTAGAAGCTACAATTAAAGGCACATTTACA
AATTTAGACACTCAAATAGATGAAGCATGGATTTTTTGGCATGCTTTATCCGCCCACAATA
CAAGTTATTATTATAATATTTTATTTTCTATTCAAAATGAAGATACAGGTGCAGTTATGGCA
GTATTACCTTTAGCATTTGAGGTTTCTGTGGATGTTGAAAAACAAAAAGTATTATTCTTTAC
AATAAAAGATAGTGCACGATATGAAGTTAAAATGAAAGCTTTGACTTTAGTTCAAGCTCTA
CATTCCTCTAATGCCCCAATTGTAGATATATTTAATGTTAATAACTATAATTTATACCATTC
TAATCATAAGATTATTCAAAATTTAAATTTATCGAATTGA

Appendix Figure A3 Nucleotide sequences of S159A mutant from DNA sequencing

> Cyt2Aa2_L160A

ATGTATACTAAAAATTTTAGTAATTCCAGAATGGAAGTAAAAGGTAATAACGGGTGTTCTG
CACCTATTATTAGAAAACCATTTAAACATATTGTATTAACGGTTCCATCCAGTGATTTAGAT
AATTTTAATACAGTCTTTTATGTACAACCACAATACATTAATCAGGCTCTTCATTTAGCAAA
TGCTTTTCAAGGGGCTATAGACCCACTTAATTTAAATTTCAATTTTGAAAAGGCACTCCAAA
TTGCAAATGGTATTCCTAATTCTGCAATTGTAAAAACTCTTAATCAAAGTGTTATACAGCAA
ACAGTTGAAATTTCAGTTATGGTTGAGCAACTTAAAAAGATTATTCAAGAGGTTTTAGGAC
TTGTTATTAACAGTACTAGTTTTTGGAATTCGGTAGAAGCTACAATTAAAGGCACATTTACA
AATTTAGACACTCAAATAGATGAAGCATGGATTTTTTGGCATAGTGCATCCGCCCACAATA
CAAGTTATTATTATAATATTTTATTTTCTATTCAAAATGAAGATACAGGTGCAGTTATGGCA
GTATTACCTTTAGCATTTGAGGTTTCTGTGGATGTTGAAAAACAAAAAGTATTATTCTTTAC
AATAAAAGATAGTGCACGATATGAAGTTAAAATGAAAGCTTTGACTTTAGTTCAAGCTCTA
CATTCCTCTAATGCCCCAATTGTAGATATATTTAATGTTAATAACTATAATTTATACCATTC
TAATCATAAGATTATTCAAAATTTAAATTTATCGAATTGA

Appendix Figure A4 Nucleotide sequences of L160A mutant from DNA sequencing

Copyright by Kasetsart University All rights reserved

> Cyt2Aa2_S161A

ATGTATACTAAAAATTTTAGTAATTCCAGAATGGAAGTAAAAGGTAATAACGGGTGTTCTG
CACCTATTATTAGAAAACCATTTAAACATATTGTATTAACGGTTCCATCCAGTGATTTAGAT
AATTTTAATACAGTCTTTTATGTACAACCACAATACATTAATCAGGCTCTTCATTTAGCAAA
TGCTTTTCAAGGGGCTATAGACCCACTTAATTTAAATTTCAATTTTGAAAAGGCACTCCAAA
TTGCAAATGGTATTCCTAATTCTGCAATTGTAAAAACTCTTAATCAAAGTGTTATACAGCAA
ACAGTTGAAATTTCAGTTATGGTTGAGCAACTTAAAAAGATTATTCAAGAGGTTTTAGGAC
TTGTTATTAACAGTACTAGTTTTTGGAATTCGGTAGAAGCTACAATTAAAGGCACATTTACA
AATTTAGACACTCAAATAGATGAAGCATGGATTTTTTGGCATAGTTTAGCCGCCCACAATA
CAAGTTATTATTATAATATTTTATTTTCTATTCAAAATGAAGATACAGGTGCAGTTATGGCA
GTATTACCTTTAGCATTTGAGGTTTCTGTGGATGTTGAAAAACAAAAAGTATTATTCTTTAC
AATAAAAGATAGTGCACGATATGAAGTTAAAATGAAAGCTTTGACTTTAGTTCAAGCTCTA
CATTCCTCTAATGCCCCAATTGTAGATATATTTAATGTTAATAACTATAATTTATACCATTC
TAATCATAAGATTATTCAAAATTTAAATTTATCGAATTGA

Appendix Figure A5 Nucleotide sequences of S161A mutant from DNA sequencing

> Cyt2Aa2_A162V

ATGTATACTAAAAATTTTAGTAATTCCAGAATGGAAGTAAAAGGTAATAACGGGTGTTCTG
CACCTATTATTAGAAAACCATTTAAACATATTGTATTAACGGTTCCATCCAGTGATTTAGAT
AATTTTAATACAGTCTTTTATGTACAACCACAATACATTAATCAGGCTCTTCATTTAGCAAA
TGCTTTTCAAGGGGCTATAGACCCACTTAATTTAAATTTCAATTTTGAAAAGGCACTCCAAA
TTGCAAATGGTATTCCTAATTCTGCAATTGTAAAAACTCTTAATCAAAGTGTTATACAGCAA
ACAGTTGAAATTTCAGTTATGGTTGAGCAACTTAAAAAGATTATTCAAGAGGTTTTAGGAC
TTGTTATTAACAGTACTAGTTTTTGGAATTCGGTAGAAGCTACAATTAAAGGCACATTTACA
AATTTAGACACTCAAATAGATGAAGCATGGATTTTTTGGCATAGTTTATCCGTACACAATA
CAAGTTATTATTATAATATTTTATTTTCTATTCAAAATGAAGATACAGGTGCAGTTATGGCA
GTATTACCTTTAGCATTTGAGGTTTCTGTGGATGTTGAAAAACAAAAAGTATTATTCTTTAC
AATAAAAGATAGTGCACGATATGAAGTTAAAATGAAAGCTTTGACTTTAGTTCAAGCTCTA
CATTCCTCTAATGCCCCAATTGTAGATATATTTAATGTTAATAACTATAATTTATACCATTC
TAATCATAAGATTATTCAAAATTTAAATTTATCGAATTGA

Appendix Figure A6 Nucleotide sequences of A162V mutant from DNA sequencing

Copyright by Kasetsart University All rights reserved

>Cyt2Aa2_D209N

ATGTATACTAAAAATTTTAGTAATTCCAGAATGGAAGTAAAAGGTAATAACGGGTGTTCTG
CACCTATTATTAGAAAACCATTTAAACATATTGTATTAACGGTTCCATCCAGTGATTTAGAT
AATTTTAATACAGTCTTTTATGTACAACCACAATACATTAATCAGGCTCTTCATTTAGCAAA
TGCTTTTCAAGGGGCTATAGACCCACTTAATTTAAATTTCAATTTTGAAAAGGCACTCCAAA
TTGCAAATGGTATTCCTAATTCTGCAATTGTAAAAACTCTTAATCAAAGTGTTATACAGCAA
ACAGTTGAAATTTCAGTTATGGTTGAGCAACTTAAAAAGATTATTCAAGAGGTTTTAGGAC
TTGTTATTAACAGTACTAGTTTTTGGAATTCGGTAGAAGCTACAATTAAAGGCACATTTACA
AATTTAGACACTCAAATAGATGAAGCATGGATTTTTTGGCATAGTTTATCCGCCCACAATA
CAAGTTATTATTATAATATTTTATTTTCTATTCAAAATGAAGATACAGGTGCAGTTATGGCA
GTATTACCTTTAGCATTTGAGGTTTCTGTGGATGTTGAAAAACAAAAAGTATTATTCTTTAC
AATAAAAAATAGTGCACGATATGAAGTTAAAATGAAAGCTTTGACTTTAGTTCAAGCTCTA
CATTCCTCTAATGCCCCAATTGTAGATATATTTAATGTTAATAACTATAATTTATACCATTC
TAATCATAAGATTATTCAAAATTTAAATTTATCGAATTGA

Appendix Figure A7 Nucleotide sequences of D209N mutant from DNA sequencing

> Cyt2Aa2_V215A

ATGTATACTAAAAATTTTAGTAATTCCAGAATGGAAGTAAAAGGTAATAACGGGTGTTCTG
CACCTATTATTAGAAAACCATTTAAACATATTGTATTAACGGTTCCATCCAGTGATTTAGAT
AATTTTAATACAGTCTTTTATGTACAACCACAATACATTAATCAGGCTCTTCATTTAGCAAA
TGCTTTTCAAGGGGCTATAGACCCACTTAATTTAAATTTCAATTTTGAAAAGGCACTCCAAA
TTGCAAATGGTATTCCTAATTCTGCAATTGTAAAAACTCTTAATCAAAGTGTTATACAGCAA
ACAGTTGAAATTTCAGTTATGGTTGAGCAACTTAAAAAGATTATTCAAGAGGTTTTAGGAC
TTGTTATTAACAGTACTAGTTTTTGGAATTCGGTAGAAGCTACAATTAAAGGCACATTTACA
AATTTAGACACTCAAATAGATGAAGCATGGATTTTTTGGCATAGTTTATCCGCCCACAATA
CAAGTTATTATTATAATATTTTATTTTCTATTCAAAATGAAGATACAGGTGCAGTTATGGCA
GTATTACCTTTAGCATTTGAGGTTTCTGTGGATGTTGAAAAACAAAAAGTATTATTCTTTAC
AATAAAAGATAGTGCACGATATGAAGCTAAAATGAAAGCTTTGACTTTAGTTCAAGCTCTA
CATTCCTCTAATGCCCCAATTGTAGATATATTTAATGTTAATAACTATAATTTATACCATTC
TAATCATAAGATTATTCAAAATTTAAATTTATCGAATTGA

Appendix Figure A8 Nucleotide sequences of V215A mutant from DNA sequencing

Copyright by Kasetsart University All rights reserved

Appendix B

Multiple sequence alignment results

Copyright by Kasetsart University All rights reserved

```
Cyt2Aa2_WT        ATGTATACTAAAAATTTTAGTAATTCCAGAATGGAAGTAAAAGGTAATAACGGGTGTTCT 60
Cyt2Aa2_I39A      ATGTATACTAAAAATTTTAGTAATTCCAGAATGGAAGTAAAAGGTAATAACGGGTGTTCT 60
Cyt2Aa2_S159A     ATGTATACTAAAAATTTTAGTAATTCCAGAATGGAAGTAAAAGGTAATAACGGGTGTTCT 60
Cyt2Aa2_L160A     ATGTATACTAAAAATTTTAGTAATTCCAGAATGGAAGTAAAAGGTAATAACGGGTGTTCT 60
Cyt2Aa2_S161A     ATGTATACTAAAAATTTTAGTAATTCCAGAATGGAAGTAAAAGGTAATAACGGGTGTTCT 60
Cyt2Aa2_A162V     ATGTATACTAAAAATTTTAGTAATTCCAGAATGGAAGTAAAAGGTAATAACGGGTGTTCT 60
Cyt2Aa2_D209N     ATGTATACTAAAAATTTTAGTAATTCCAGAATGGAAGTAAAAGGTAATAACGGGTGTTCT 60
Cyt2Aa2_V215A     ATGTATACTAAAAATTTTAGTAATTCCAGAATGGAAGTAAAAGGTAATAACGGGTGTTCT 60
                  ************************************************************

Cyt2Aa2_WT        GCACCTATTATTAGAAAACCATTTAAACATATTGTATTAACGGTTCCATCCAGTGATTTA 120
Cyt2Aa2_I39A      GCACCTATTATTAGAAAACCATTTAAACATATTGTATTAACGGTTCCATCCAGTGATTTA 120
Cyt2Aa2_S159A     GCACCTATTATTAGAAAACCATTTAAACATATTGTATTAACGGTTCCATCCAGTGATTTA 120
Cyt2Aa2_L160A     GCACCTATTATTAGAAAACCATTTAAACATATTGTATTAACGGTTCCATCCAGTGATTTA 120
Cyt2Aa2_S161A     GCACCTATTATTAGAAAACCATTTAAACATATTGTATTAACGGTTCCATCCAGTGATTTA 120
Cyt2Aa2_A162V     GCACCTATTATTAGAAAACCATTTAAACATATTGTATTAACGGTTCCATCCAGTGATTTA 120
Cyt2Aa2_D209N     GCACCTATTATTAGAAAACCATTTAAACATATTGTATTAACGGTTCCATCCAGTGATTTA 120
Cyt2Aa2_V215A     GCACCTATTATTAGAAAACCATTTAAACATATTGTATTAACGGTTCCATCCAGTGATTTA 120
                  ************************************************************

Cyt2Aa2_WT        GATAATTTTAATACAGTCTTTTATGTACAACCACAATACATTAATCAGGCTCTTCATTTA 180
Cyt2Aa2_I39A      GATAATTTTAATACAGTCTTTTATGTACAACCACAATACATTAATCAGGCTCTTCATTTA 180
Cyt2Aa2_S159A     GATAATTTTAATACAGTCTTTTATGTACAACCACAATACATTAATCAGGCTCTTCATTTA 180
Cyt2Aa2_L160A     GATAATTTTAATACAGTCTTTTATGTACAACCACAATACATTAATCAGGCTCTTCATTTA 180
Cyt2Aa2_S161A     GATAATTTTAATACAGTCTTTTATGTACAACCACAATACATTAATCAGGCTCTTCATTTA 180
Cyt2Aa2_A162V     GATAATTTTAATACAGTCTTTTATGTACAACCACAATACATTAATCAGGCTCTTCATTTA 180
Cyt2Aa2_D209N     GATAATTTTAATACAGTCTTTTATGTACAACCACAATACATTAATCAGGCTCTTCATTTA 180
Cyt2Aa2_V215A     GATAATTTTAATACAGTCTTTTATGTACAACCACAATACATTAATCAGGCTCTTCATTTA 180
                  ************************************************************

Cyt2Aa2_WT        GCAAATGCTTTTCAAGGGGCTATAGACCCACTTAATTTAAATTTCAATTTTGAAAAGGCA 240
Cyt2Aa2_I39A      GCAAATGCTTTTCAAGGGGCTATAGACCCACTTAATTTAAATTTCAATTTTGAAAAGGCA 240
Cyt2Aa2_S159A     GCAAATGCTTTTCAAGGGGCTATAGACCCACTTAATTTAAATTTCAATTTTGAAAAGGCA 240
Cyt2Aa2_L160A     GCAAATGCTTTTCAAGGGGCTATAGACCCACTTAATTTAAATTTCAATTTTGAAAAGGCA 240
Cyt2Aa2_S161A     GCAAATGCTTTTCAAGGGGCTATAGACCCACTTAATTTAAATTTCAATTTTGAAAAGGCA 240
Cyt2Aa2_A162V     GCAAATGCTTTTCAAGGGGCTATAGACCCACTTAATTTAAATTTCAATTTTGAAAAGGCA 240
Cyt2Aa2_D209N     GCAAATGCTTTTCAAGGGGCTATAGACCCACTTAATTTAAATTTCAATTTTGAAAAGGCA 240
Cyt2Aa2_V215A     GCAAATGCTTTTCAAGGGGCTATAGACCCACTTAATTTAAATTTCAATTTTGAAAAGGCA 240
                  ************************************************************

Cyt2Aa2_WT        CTCCAAATTGCAAATGGTATTCCTAATTCTGCAATTGTAAAAACTCTTAATCAAAGTGTT 300
Cyt2Aa2_I39A      CTCCAAATTGCAAATGGTATTCCTAATTCTGCAATTGTAAAAACTCTTAATCAAAGTGTT 300
Cyt2Aa2_S159A     CTCCAAATTGCAAATGGTATTCCTAATTCTGCAATTGTAAAAACTCTTAATCAAAGTGTT 300
Cyt2Aa2_L160A     CTCCAAATTGCAAATGGTATTCCTAATTCTGCAATTGTAAAAACTCTTAATCAAAGTGTT 300
Cyt2Aa2_S161A     CTCCAAATTGCAAATGGTATTCCTAATTCTGCAATTGTAAAAACTCTTAATCAAAGTGTT 300
Cyt2Aa2_A162V     CTCCAAATTGCAAATGGTATTCCTAATTCTGCAATTGTAAAAACTCTTAATCAAAGTGTT 300
Cyt2Aa2_D209N     CTCCAAATTGCAAATGGTATTCCTAATTCTGCAATTGTAAAAACTCTTAATCAAAGTGTT 300
Cyt2Aa2_V215A     CTCCAAATTGCAAATGGTATTCCTAATTCTGCAATTGTAAAAACTCTTAATCAAAGTGTT 300
                  ************************************************************

Cyt2Aa2_WT        ATACAGCAAACAGTTGAAATTTCAGTTATGGTTGAGCAACTTAAAAAGATTATTCAAGAG 360
Cyt2Aa2_I39A      ATACAGCAAACAGTTGAAATTTCAGTTATGGTTGAGCAACTTAAAAAGATTATTCAAGAG 360
Cyt2Aa2_S159A     ATACAGCAAACAGTTGAAATTTCAGTTATGGTTGAGCAACTTAAAAAGATTATTCAAGAG 360
Cyt2Aa2_L160A     ATACAGCAAACAGTTGAAATTTCAGTTATGGTTGAGCAACTTAAAAAGATTATTCAAGAG 360
Cyt2Aa2_S161A     ATACAGCAAACAGTTGAAATTTCAGTTATGGTTGAGCAACTTAAAAAGATTATTCAAGAG 360
Cyt2Aa2_A162V     ATACAGCAAACAGTTGAAATTTCAGTTATGGTTGAGCAACTTAAAAAGATTATTCAAGAG 360
Cyt2Aa2_D209N     ATACAGCAAACAGTTGAAATTTCAGTTATGGTTGAGCAACTTAAAAAGATTATTCAAGAG 360
Cyt2Aa2_V215A     ATACAGCAAACAGTTGAAATTTCAGTTATGGTTGAGCAACTTAAAAAGATTATTCAAGAG 360
                  ************************************************************
```

Appendix Figure B1 The sequnce alignment of Cyt2Aa2 wild type and all mutant by ClustalW2 and high-lighted mutated nucleotide positions

Copyright by Kasetsart University All rights reserved

```
Cyt2Aa2_WT          GTTTTAGGACTTGTTATTAACAGTACTAGTTTTTGGAATTCGGTAGAAGCTACAATTAAA 420
Cyt2Aa2_I39A        GTTTTAGGACTTGTTATTAACAGTACTAGTTTTTGGAATTCGGTAGAAGCTACAGCTAAA 420
Cyt2Aa2_S159A       GTTTTAGGACTTGTTATTAACAGTACTAGTTTTTGGAATTCGGTAGAAGCTACAATTAAA 420
Cyt2Aa2_L160A       GTTTTAGGACTTGTTATTAACAGTACTAGTTTTTGGAATTCGGTAGAAGCTACAATTAAA 420
Cyt2Aa2_S161A       GTTTTAGGACTTGTTATTAACAGTACTAGTTTTTGGAATTCGGTAGAAGCTACAATTAAA 420
Cyt2Aa2_A162V       GTTTTAGGACTTGTTATTAACAGTACTAGTTTTTGGAATTCGGTAGAAGCTACAATTAAA 420
Cyt2Aa2_D209N       GTTTTAGGACTTGTTATTAACAGTACTAGTTTTTGGAATTCGGTAGAAGCTACAATTAAA 420
Cyt2Aa2_V215A       GTTTTAGGACTTGTTATTAACAGTACTAGTTTTTGGAATTCGGTAGAAGCTACAATTAAA 420
                    ************************************************************

Cyt2Aa2_WT          GGCACATTTACAAATTTAGACACTCAAATAGATGAAGCATGGATTTTTTGGCATAGTTTA 480
Cyt2Aa2_I39A        GGCACATTTACAAATTTAGACACTCAAATAGATGAAGCATGGATTTTTTGGCATAGTTTA 480
Cyt2Aa2_S159A       GGCACATTTACAAATTTAGACACTCAAATAGATGAAGCATGGATTTTTTGGCATGCTTTA 480
Cyt2Aa2_L160A       GGCACATTTACAAATTTAGACACTCAAATAGATGAAGCATGGATTTTTTGGCATAGTGCA 480
Cyt2Aa2_S161A       GGCACATTTACAAATTTAGACACTCAAATAGATGAAGCATGGATTTTTTGGCATAGTTTA 480
Cyt2Aa2_A162V       GGCACATTTACAAATTTAGACACTCAAATAGATGAAGCATGGATTTTTTGGCATAGTTTA 480
Cyt2Aa2_D209N       GGCACATTTACAAATTTAGACACTCAAATAGATGAAGCATGGATTTTTTGGCATAGTTTA 480
Cyt2Aa2_V215A       GGCACATTTACAAATTTAGACACTCAAATAGATGAAGCATGGATTTTTTGGCATAGTTTA 480
                    ************************************************************

Cyt2Aa2_WT          TCCGCCCACAATACAAGTTATTATTATAATATTTTATTTTCTATTCAAAATGAAGATACA 540
Cyt2Aa2_I39A        TCCGCCCACAATACAAGTTATTATTATAATATTTTATTTTCTATTCAAAATGAAGATACA 540
Cyt2Aa2_S159A       TCCGCCCACAATACAAGTTATTATTATAATATTTTATTTTCTATTCAAAATGAAGATACA 540
Cyt2Aa2_L160A       TCCGCCCACAATACAAGTTATTATTATAATATTTTATTTTCTATTCAAAATGAAGATACA 540
Cyt2Aa2_S161A       GCCGCCCACAATACAAGTTATTATTATAATATTTTATTTTCTATTCAAAATGAAGATACA 540
Cyt2Aa2_A162V       TCCGTACACAATACAAGTTATTATTATAATATTTTATTTTCTATTCAAAATGAAGATACA 540
Cyt2Aa2_D209N       TCCGCCCACAATACAAGTTATTATTATAATATTTTATTTTCTATTCAAAATGAAGATACA 540
Cyt2Aa2_V215A       TCCGCCCACAATACAAGTTATTATTATAATATTTTATTTTCTATTCAAAATGAAGATACA 540
                     ***  ************************************************************

Cyt2Aa2_WT          GGTGCAGTTATGGCAGTATTACCTTTAGCATTTGAGGTTTCTGTGGATGTTGAAAAACAA 600
Cyt2Aa2_I39A        GGTGCAGTTATGGCAGTATTACCTTTAGCATTTGAGGTTTCTGTGGATGTTGAAAAACAA 600
Cyt2Aa2_S159A       GGTGCAGTTATGGCAGTATTACCTTTAGCATTTGAGGTTTCTGTGGATGTTGAAAAACAA 600
Cyt2Aa2_L160A       GGTGCAGTTATGGCAGTATTACCTTTAGCATTTGAGGTTTCTGTGGATGTTGAAAAACAA 600
Cyt2Aa2_S161A       GGTGCAGTTATGGCAGTATTACCTTTAGCATTTGAGGTTTCTGTGGATGTTGAAAAACAA 600
Cyt2Aa2_A162V       GGTGCAGTTATGGCAGTATTACCTTTAGCATTTGAGGTTTCTGTGGATGTTGAAAAACAA 600
Cyt2Aa2_D209N       GGTGCAGTTATGGCAGTATTACCTTTAGCATTTGAGGTTTCTGTGGATGTTGAAAAACAA 600
Cyt2Aa2_V215A       GGTGCAGTTATGGCAGTATTACCTTTAGCATTTGAGGTTTCTGTGGATGTTGAAAAACAA 600
                    ************************************************************

Cyt2Aa2_WT          AAAGTATTATTCTTTACAATAAAAGATAGTGCACGATATGAAGTTAAAATGAAAGCTTTG 660
Cyt2Aa2_I39A        AAAGTATTATTCTTTACAATAAAAGATAGTGCACGATATGAAGTTAAAATGAAAGCTTTG 660
Cyt2Aa2_S159A       AAAGTATTATTCTTTACAATAAAAGATAGTGCACGATATGAAGTTAAAATGAAAGCTTTG 660
Cyt2Aa2_L160A       AAAGTATTATTCTTTACAATAAAAGATAGTGCACGATATGAAGTTAAAATGAAAGCTTTG 660
Cyt2Aa2_S161A       AAAGTATTATTCTTTACAATAAAAGATAGTGCACGATATGAAGTTAAAATGAAAGCTTTG 660
Cyt2Aa2_A162V       AAAGTATTATTCTTTACAATAAAAGATAGTGCACGATATGAAGTTAAAATGAAAGCTTTG 660
Cyt2Aa2_D209N       AAAGTATTATTCTTTACAATAAAAAATAGTGCACGATATGAAGTTAAAATGAAAGCTTTG 660
Cyt2Aa2_V215A       AAAGTATTATTCTTTACAATAAAAGATAGTGCACGATATGAAGCTAAAATGAAAGCTTTG 660
                    ********************** ********** ********** **********

Cyt2Aa2_WT          ACTTTAGTTCAAGCTCTACATTCCTCTAATGCCCCAATTGTAGATATATTTAATGTTAAT 720
Cyt2Aa2_I39A        ACTTTAGTTCAAGCTCTACATTCCTCTAATGCCCCAATTGTAGATATATTTAATGTTAAT 720
Cyt2Aa2_S159A       ACTTTAGTTCAAGCTCTACATTCCTCTAATGCCCCAATTGTAGATATATTTAATGTTAAT 720
Cyt2Aa2_L160A       ACTTTAGTTCAAGCTCTACATTCCTCTAATGCCCCAATTGTAGATATATTTAATGTTAAT 720
Cyt2Aa2_S161A       ACTTTAGTTCAAGCTCTACATTCCTCTAATGCCCCAATTGTAGATATATTTAATGTTAAT 720
Cyt2Aa2_A162V       ACTTTAGTTCAAGCTCTACATTCCTCTAATGCCCCAATTGTAGATATATTTAATGTTAAT 720
Cyt2Aa2_D209N       ACTTTAGTTCAAGCTCTACATTCCTCTAATGCCCCAATTGTAGATATATTTAATGTTAAT 720
Cyt2Aa2_V215A       ACTTTAGTTCAAGCTCTACATTCCTCTAATGCCCCAATTGTAGATATATTTAATGTTAAT 720
                    ************************************************************
```

Appendix Figure B1 (Continued)

Copyright by Kasetsart University All rights reserved

```
Cyt2Aa2_WT        AACTATAATTTATACCATTCTAATCATAAGATTATTCAAAATTTAAATTTATCGAATTGA 780
Cyt2Aa2_I39A      AACTATAATTTATACCATTCTAATCATAAGATTATTCAAAATTTAAATTTATCGAATTGA 780
Cyt2Aa2_S159A     AACTATAATTTATACCATTCTAATCATAAGATTATTCAAAATTTAAATTTATCGAATTGA 780
Cyt2Aa2_L160A     AACTATAATTTATACCATTCTAATCATAAGATTATTCAAAATTTAAATTTATCGAATTGA 780
Cyt2Aa2_S161A     AACTATAATTTATACCATTCTAATCATAAGATTATTCAAAATTTAAATTTATCGAATTGA 780
Cyt2Aa2_A162V     AACTATAATTTATACCATTCTAATCATAAGATTATTCAAAATTTAAATTTATCGAATTGA 780
Cyt2Aa2_D209N     AACTATAATTTATACCATTCTAATCATAAGATTATTCAAAATTTAAATTTATCGAATTGA 780
Cyt2Aa2_V215A     AACTATAATTTATACCATTCTAATCATAAGATTATTCAAAATTTAAATTTATCGAATTGA 780
                  ************************************************************
```

Appendix Figure B1 (Continued)

Copyright by Kasetsart University All rights reserved

Appendix C

Interaction of Cyt2Aa2 toxin

Copyright by Kasetsart University All rights reserved

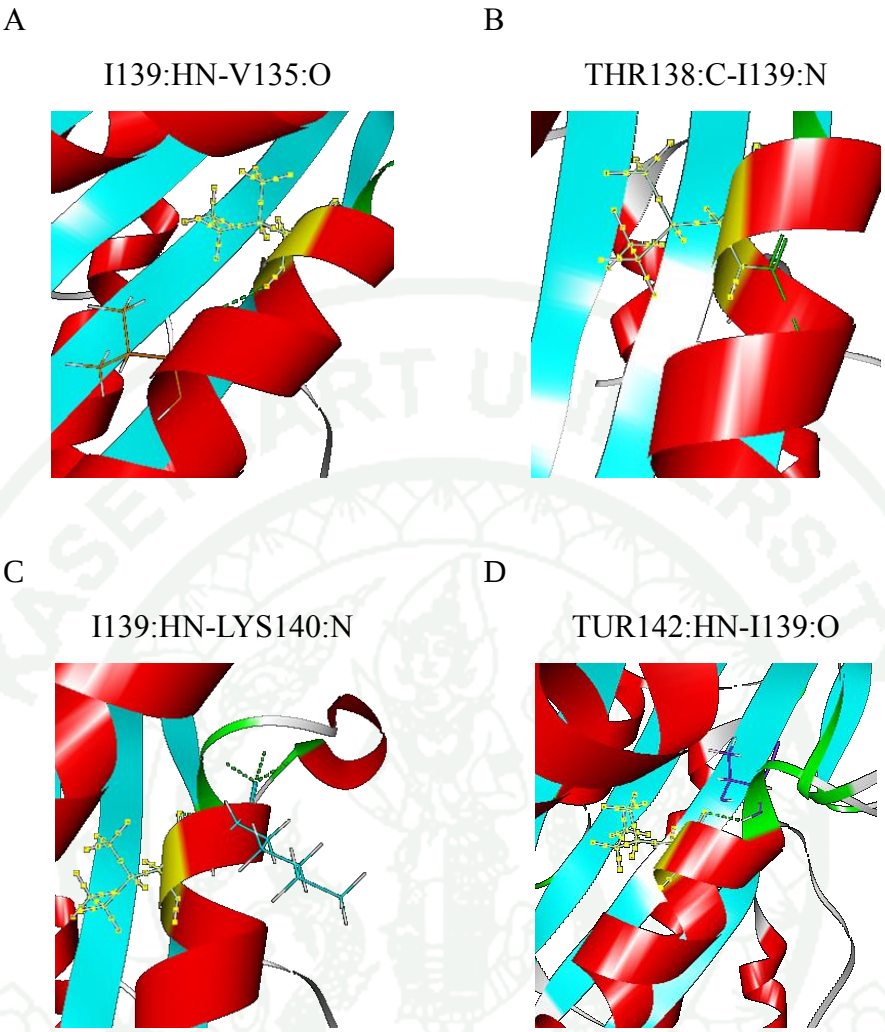

Appendix Figure C1 Interaction of Cyt2Aa2 toxin at I139. A) H-atom from amino group of I139 interacts with O-atom of V135 by hydrogen bond. B) H-atom from C-carbon backbone of THR138 interacts with N-atom of I139 by hydrogen bond. C) H-atom from amino group of I139 interacts with N-atom of LYS140 by hydrogen bond. D) H-atom from amino group of TUR142 interacts with O-atom of I139 by hydrogen bond.

Copyright by Kasetsart University All rights reserved

HIS158:ND1-SER159:OG

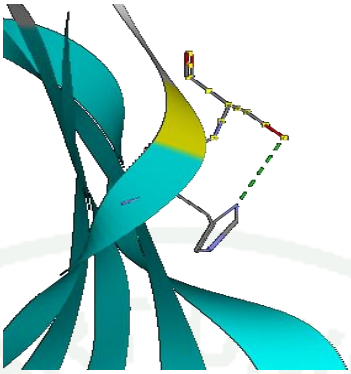

Appendix Figure C2 Interaction of Cyt2Aa2 toxin at S159. N-atom from side chain of HIS158 interacts with O-atom from side chain of SER159 by hydrogen bond.

A

LUE160:HD1-HIS158:O

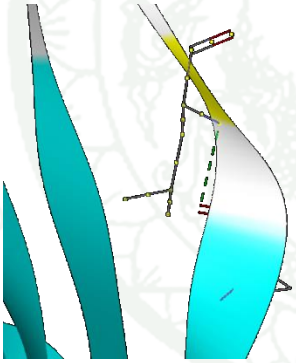

B

SER161:OG-LUE160:O

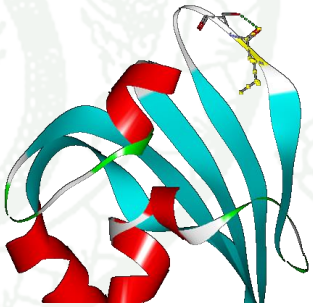

Appendix Figure C3 Interaction of Cyt2Aa2 toxin at L160. A) H-atom from C-backbone interacts with O-atom from carboxyl group of HIS158 by hydrogen bond. B) O-atom from side chain of SER161 interacts with O-atom from carboxyl group of LUE160 by hydrogen bond.

Copyright by Kasetsart University All rights reserved

A SER161:OG-LUE160:O

B SER161:N-ASN164:O

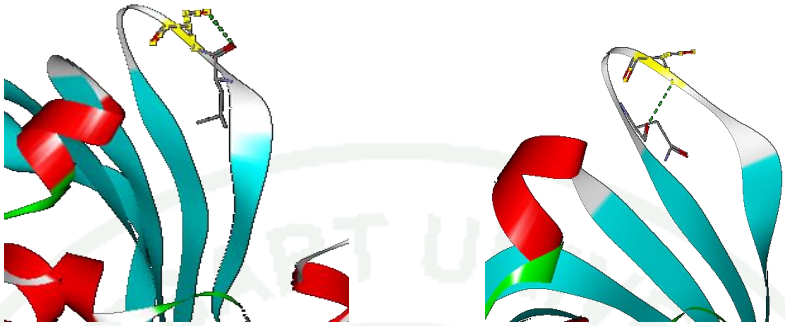

Appendix Figure C4 Interaction of Cyt2Aa2 toxin at S161. A) O-atom from side chain of SER161 interacts with O-atom of LUE160 by hydrogen bond. B) N-atom of SER161 interacts with O-atom from carboxyl group of ASN164 by hydrogen bond.

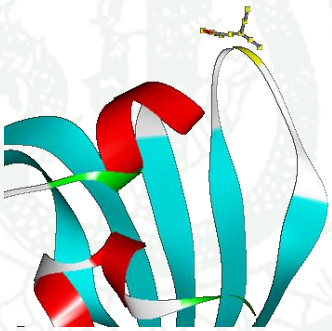

Appendix Figure C5 Interaction of Cyt2Aa2 toxin at A162 and other residue is not occurred.

Copyright by Kasetsart University All rights reserved

ASP209:N-THR206:O

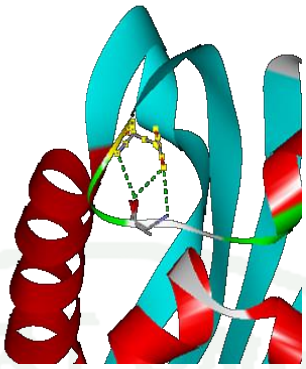

Appendix Figure C6 Interaction of Cyt2Aa2 toxin at D209. N-atom of ASP209 interacts with O-atom from carboxyl group of THR206 by hydrogen bond.

A

VAL215:N-ILE101:O

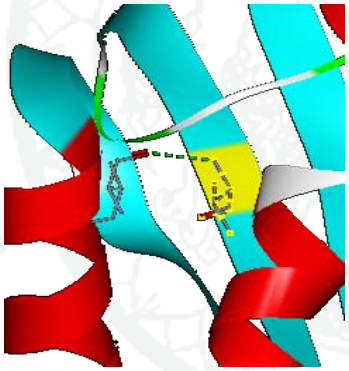

B

VAL215:N-GLU214:OE2

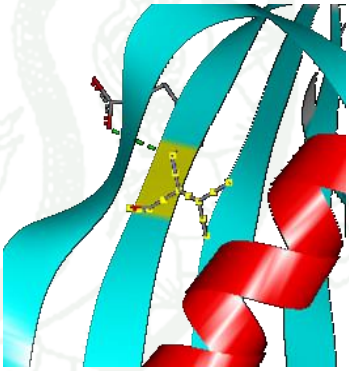

Appendix Figure C7 Interaction of Cyt2Aa2 toxin at V215. A) N-atom of VAL215 interacts with O-atom of ILE101 by hydrogen bond. B) N-atom of VAL215 interacts with O-atom from side chain of GLU214 by hydrogen bond.

Copyright by Kasetsart University All rights reserved

CURRICULUM VITAE

NAME : Miss. Pajaree Saitonuang

BIRTH DATE : October 18, 1989

BIRTH PLACE : Phatthalung, Thailand

EDUCATION :

YEAR	**INSTITUTE**	**DEGREE/DIPLOMA**
2012	Kasetsart University	B.S. (Biology)

SCHOLARSHIP : Thailand Graduate Institute of Science and Technology (TGIST)

Copyright by Kasetsart University All rights reserved